



รายงานวิจัยฉบับสมบูรณ์

โครงการ การคุ้ดชับหนองนิลฟินอลโดยใช้ชีวมวลตรึงที่ไร้ชีวิตของฟังไจ

โดย ดร.วีราณุช หลาง

กรกฎาคม 2552

สัญญาเลขที่ MRG5080420

รายงานวิจัยฉบับสมบูรณ์

โครงการ การดูดซับหนองน้ำลีฟนอลโดยใช้ชีวมวลตรึงที่ไร้ชีวิตของฟังไจ

ดร.วีระนุช หลาง
สาขาวิชาจุลชีววิทยาเกษตรและสิ่งแวดล้อม
โครงการจัดตั้งสาขาวิชาจุลชีววิทยา[†]
คณะศิลปศาสตร์และวิทยาศาสตร์
มหาวิทยาลัยเกษตรศาสตร์ วิทยาเขตกำแพงแสน

สนับสนุนโดยสำนักงานกองทุนสนับสนุนการวิจัย
(ความเห็นในรายงานนี้เป็นของผู้วิจัย สกาว. ไม่จำเป็นต้องเห็นด้วยเสมอไป)

กิตติกรรมประกาศ

ผู้วิจัยขอขอบพระคุณ ศาสตราจารย์ ดร.โนบุโอะ ชาガอิริ แห่ง Graduate school of Environmental Earth Science มหาวิทยาลัยออกไกโอด ประเทศญี่ปุ่น และ รองศาสตราจารย์ ดร. สารโจน์ ศิริคันสน์ยิกุล ภาควิชาเทคโนโลยีชีวภาพ คณะอุตสาหกรรมเกษตร อาจารย์ที่ปรึกษา โครงการวิจัยที่ได้กรุณาให้คำปรึกษา คำแนะนำ และตรวจแก้ไขผลงานในการทำวิจัยครั้งนี้

ขอขอบคุณ สำนักงานกองทุนสนับสนุนการวิจัย ที่ให้ทุนวิจัยประเภท ทุนพัฒนาศักยภาพ ของอาจารย์รุ่นใหม่ ประจำปี 2550-2551 หมายเลขโครงการ MRG 5080420 และมีระบบการจัด ประการการเป็นนักวิจัยมืออาชีพให้กับอาจารย์รุ่นใหม่ ๆ

ขอขอบคุณ โครงการอุดสาหกรรมและวิจัยสำหรับนักศึกษาปริญญาตรี IRPUS ประเภท RPUS หมายเลขโครงการ R51A13001 ที่ให้ทุนการศึกษาสำหรับนิสิตผู้ช่วยวิจัยและมีเวทีให้นิสิต นำเสนอผลงานและแลกเปลี่ยนประสบการณ์งานวิจัยกับภาควิชาอุตสาหกรรม

ขอขอบคุณ ผู้ช่วยศาสตราจารย์ ดร.ชานันก์ สุดสุข คณะดีคณศิลปศาสตร์และวิทยา ศาสตร์ ผู้เกื้อหนุนสภาพแวดล้อมในการทำงานและแนวคิดในการทำงานบริหารความคุ้มกับการเป็นนัก วิจัย

ขอขอบคุณครูปراسาร ชิวปรีชา เจ้าหน้าที่ในโครงการจัดตั้งสาขาวิชาจุลชีววิทยา ที่ให้ความ สะดวกสำหรับอุปกรณ์และสถานที่ในการทำวิจัย

ขอขอบคุณอาจารย์ Wilhelm J. Holzschuh ที่ช่วยตรวจแก้ไขภาษาอังกฤษของต้นฉบับ งานวิจัยดีมิท

ขอกราบขอบพระคุณมารดา และขอบคุณบุคคลในครอบครัวที่เป็นแรงบันดาลใจและกำลัง ใจที่อบอุ่น

วีรานุช หลาง

กรกฎาคม 2552

บทคัดย่อ

รหัสโครงการ : MRG 5080420

ชื่อโครงการ : การดูดซับอนิลฟีนอลโดยใช้ชีวมวลตระกูลไรซีวิตของพังไจ

ชื่อนักวิจัย : วีรานุช หลาง

สาขาวิชาจุลชีววิทยาเกษตรและสิ่งแวดล้อม โครงการจัดตั้งสายวิชาจุลชีววิทยา
คณะศิลปศาสตร์และวิทยาศาสตร์ มหาวิทยาลัยเกษตรศาสตร์ 73140

E-mail address : faaswnp@ku.ac.th, we_era@hotmail.com

ระยะเวลาโครงการ : 1 กรกฎาคม 2550 – 2 กรกฎาคม 2552 (2 ปี)

งานวิจัยนี้ศึกษาไออกซ์เทอમและแบบจำลอง込んでลดเวลาการดูดซับและการคายสารอนิลฟีนอลด้วยมวลชีวภาพราที่เจริญโดยใช้โคโตชาณเป็นวัสดุพยุง มวลชีวภาพตระกูลไรซีวิตของเส้นไบร้า *Rhizopus arrhizus* TISTR3610 มีประสิทธิภาพสูงสุดในการดูดซับอนิลฟีนอลซึ่งเป็นสารเคมีกลุ่มที่รบกวนการทำงานของต่อมไร้ท่อ ภาพถ่ายจากกล้องจุลทรรศน์อิเล็กตรอนแสดงให้เห็นว่าเส้นไบร้าเจริญแพร่กระจายภายในและเจริญปักคลุมรอบผิวของเม็ดเจลไคโตชาณ การทดสอบการดูดซับสารอนิลฟีนอลด้วยเม็ดราตรีงไรซีวิตที่เจริญในไคโตชาณในระบบเบ็ดเสร็จที่ความเข้มข้นของอนิลฟีนอลเริ่มต้น $20.12 \text{ ถึง } 245.15$ มิลลิกรัมต่อลิตร พบร่วมกับการดูดซับที่ภาวะสมดุลสอดคล้องกับไออกซ์เทอમของฟริทซ์-ชาวเดอร์มากกว่าไออกซ์เทอມของเรดลิก-เพเทอร์สัน และเมียร์และฟรอยลิก โดยใช้ไรซีวิเคราะห์แบบถดถอยไม่เชิงเส้นด้วย solver add-in จากโปรแกรมไมโครซอฟท์เอ็กซ์เซล การศึกษาการแพร่ภายในของสารอนิลฟีนอลเข้าสู่เม็ดราตรีงไรซีวิตโดยใช้แบบจำลองแกนหดตัวคำนวณค่าอัตราการแพร่ภายในอยู่ในอุปกรณ์ช่วง $2.3736 \times 10^{-4} - 1.8950 \times 10^{-4}$ ตารางเซนติเมตร/วินาที เม็ดราตรีงไรซีวิตมีความจำเพาะของการดูดซับสารอนิลฟีนอลสูงมากกว่าฟีนอลและ poly)ethylene glycol(4-nonylphenol-3-sulfopropyl ether, potassium salt (PSE) ที่เป็นกลุ่มสารที่มีโครงสร้างคล้ายคลึงกับอนิลฟีนอล ในการทดสอบการคายสารอนิลฟีนอลเพื่อการนำเม็ดราตรีงไรซีวิตกลับมาใช้ซ้ำโดยใช้เมทานอลเป็นสารละลายจะสามารถถอดชิบายได้ด้วยสมการ pseudo second-order ซึ่งเหมาะสมมากกว่าแบบจำลอง pore diffusion และ pseudo second-order โดยมีค่าคงที่ทาง込んでลดเวลาการดูดซับต่อนาที เม็ดราตรีงไรซีวิตที่เตรียมขึ้นนี้มีประสิทธิภาพในการนำกลับมาใช้ซ้ำได้อย่างน้อย 3 รอบ ซึ่งสามารถลดอนิลฟีนอลที่ถูกดูดซับออกได้ด้วยเมทานอลเกือบทั้งหมด

คำหลัก : การดูดซับทางชีวภาพ, อนิลฟีนอล, ไออกซ์บีส อาริชัส, ไคโตชาณ, แบบจำลองทางเ込んでลดเวลาการคายสาร

Abstract

Project Code : MRG 5080420

Project Title : Biosorption of nonylphenol on dead biomass of *Rhizopus arrhizus* encapsulated in chitosan beads.

Investigator : Weeranuch Lang

Division of Environmental and Agricultural Microbiology, Department of Microbiology, Faculty of Liberal Arts and Science, Kasetsart University, Kampaeng Saen, Nakorn-Pathom 73140, Thailand

E-mail address : faaswnp@ku.ac.th, we_era@hotmail.com

Project Period : 1 July 2007 – 2 July 2009 (2 years)

In this study, isotherm and kinetics models for nonylphenol (NP) biosorption and desorption by the fungal biomass using chitosan as a supporting material were investigated. Filamentous fungal biomass of *Rhizopus arrhizus* TISTR3610 exhibited the most potential uptake of NP, an endocrine disrupting chemicals. Scanning electron microscopy (SEM) revealed the exuberant mycelia distributed inside and on the bead surface. Biosorption of NP using the immobilized non-living fungal mycelium grown in chitosan beads was performed under batch conditions with initial NP concentrations ranging from 20.12 to 245.15 mg/L. The equilibrium adsorption data were best correlated with various adsorption isotherms in the order Fritz-Schluender, Redlich-Peterson, Langmuir, and Freundlich by using non-linear least-regression with the *solver* add-in in Microsoft Excel. The diffusivity of NP in the *R. arrhizus*-chitosan beads was calculated using the shrinking core model, and the diffusivity values were in the ranges of 2.3736×10^{-4} – 1.8950×10^{-4} $\text{cm}^2 \text{s}^{-1}$. The adsorption selectivity of the beads for NP was excellently higher than the two similar structure compounds, phenol and poly(ethylene glycol(4-nonylphenol-3-sulfopropyl ether, potassium salt (PSE). Desorption to recover the adsorbed NP from the beads was performed in methanol and was best described using a pseudo second-order kinetic model compared to pore diffusion model and pseudo first-order. The second-order desorption rate (K_{D2}) constant was determined as 0.2243 g/mg min. The regeneration of used dead beads was effective for at least 3 batch consecutive cycles which almost NP uptake could still be eluted.

Keywords: Biosorption; Nonylphenol; *Rhizopus arrhizus*; Chitosan; kinetic modelling

List of Symbols

V	volume of aqueous phase (L)
M	mass of biomass (g)
a_s	Fritz-Schlünder isotherm constant (mg/L) ^{-b2}
a_R	Redlich-Peterson isotherm constant (L/mg) ^{β}
b	Langmuir isotherm constant (L/mg)
b_1, b_2	Fritz-Schlünder isotherm constants (dimensionless)
C	concentration of NP at time, t (ppm)
C_0	initial concentration of NP (ppm)
C^0	$\frac{(C_0 - C_e)V}{n^{\frac{4}{3}} \pi R^3}$, average NP binding site density (ppm)
C_e	concentration of NP at equilibrium (ppm)
D	diffusion coefficient (cm ² /s)
K_1	Pseudo first-order rate constant (min ⁻¹)
K_2	Pseudo second-order rate constant modified (g/mg min)
k_p	intraparticle diffusion rate constant (mg/g min ^{0.5})
K_F	Freundlich constant, characteristic of the system related to the adsorption capacity (mg/g)
K_R	Redlich-Peterson isotherm constant (L/g)
K_s	Fritz-Schlünder isotherm constant (mg/g) (mg/L) ^{-b1}
n	Freundlich constant, characteristic of the system related to the adsorption intensity (dimensionless)
q	NP uptake rate (mg/g)
q_e	NP uptake rate at equilibrium (mg/g)
Q_0	Langmuir adsorption isotherm constant (mg/g) (Dependent on the maximum adsorption capacity of biosorbent)
R	radius of bead (cm)
t	contact time (min)

$X, F(X)$ Functions derived from the shrinking core model (Preetha and Viruthagirl, 2007)

RMS root mean square

q_{cal} theoretical NP uptake (mg/g)

q_{exp} experimental NP uptake (mg/g)

K_D desorption rate constant (s^{-1})

Greek letters

α $\int_0^t C dt$, derived from the shrinking core model, defined in Eq.(13) and (14) (Preetha and Viruthagirl, 2007)

α_P Redlich-Peterson isotherm constant

β Redlich-Peterson isotherm constant (Dependent on the heterogeneity of the binding surface)

1. Objectives

1. To examine the nonylphenol removal capacity of immobilized non-viable fungal biomass as a potentially low-cost sorbent by using chitosan, commercially produced by Thailand industry, as an inexpensive and abundant supporting material.
2. To study the novel alternative methods of fungal cell immobilization in chitosan sphere since chitosan is known to be anti-fungal polymer for vegetative cells.
3. To investigate the influencing factors and regeneration on nonylphenol biosorption.
4. To preliminarily study on the process scale-up for nonylphenol removal.

2. Introduction

Nonylphenol (NP) is one of the organic pollutants found in aquatic environments as a consequence of the biodegradation of nonylphenol polyethoxylate (NPnEO), a non-ionic surfactant contained in industrial cleaning products and in household detergents (Ahel *et al.*, 1993). Although the parent surfactant itself is less toxic, NPnEO released into the environment rapidly decomposes to form NP which is the most recalcitrant intermediate of NPnEO decomposition. Principally NP persists in sewage treatment plants and outflows (Nakada *et al.*, 2006), and tends to accumulate in the fatty tissue of aquatic organisms when released into aquatic environments.

NP is known to be an endocrine disruptor compound, that is, it mimics endogenous hormones and disrupts important life processes. Substantial evidence exists to demonstrate that NP causes various disorders of the male reproductive system, including reduced testicular size and lower sperm production in rainbow trout and other marine animals (Granmo *et al.*, 1989; Ekelund *et al.*, 1990). NP and NPnEO have been banned in the European Union as a hazard to human and environmental safety. However, NP and NPnEO are still widely used in Thailand and other Asian countries, especially as industrial detergents such as those used for wool washing and metal finishing, in various laboratory detergents including Titron X-100, in industrial processes such as emulsion polymerisation, and in some pesticide formulations.

Although the techniques of adsorption on activated carbon, photo-oxidation and ozone treatment for NP removal have been studied and found to be effective, cost-effectiveness is the main limitation against widespread practical use (Nevskaia and Guerrero, 2001; Kawasaki *et al.*, 2001). The search for a low cost and easily available adsorbent has led the authors to investigate materials of agricultural and biological origin, and some industrial by-products as adsorbents.

Biosorption, the passive uptake of pollutants by non-growing or non-living microbial biomass such as bacteria, fungi and algae, is considered to have good potential for the removal of non-degradable pollutants from aqueous solution (Kapoor and Viraraghavan, 1995). Reports of biosorption of toxic organic compounds with biomass showed that better removal was obtained with dead biomass than with live biomass (Aksu, 2005). Immobilisation may also allow higher biomass concentrations, and facilitate separation and non-destructive recovery of biomass from pollutant-bearing solution (Fu and Viraraghavan, 2001). Immobilised fungal biomass has been used for the removal of various metals, dyes and some organic pollutants (Kapoor and Viraraghavan, 1995; Aksu, 2005) but no study has been conducted on the use of immobilised biomass for the removal of NP or other endocrine disruptor compounds. Therefore, there is a need to study the performance of the immobilised fungus system with NP.

Chitosan, (1→4)-2-amino-2-deoxy- β -D-glucan, produced on an industrial scale by the alkaline deacetylation of chitin, one of the most abundant biopolymers in nature, was used in this study as the supporting material for living biomass immobilisation. It should be noted that the use of chitosan for living cell immobilisation has a limitation due to its anti-microbial activity (Helander *et al.*, 2001). However, the fungal resting spores used in this study are tolerant to chitosan gelling because of their extra thick cell wall.

This study presents the biosorption characteristics of NP on dead chitosan-immobilised fungal beads, referred to as "dead beads". Suitable isotherm and kinetic models fitted by non-linear regression using the 'solver' add-in with Microsoft Excel 2007 are proposed. Also, the reusability of the dead beads, that is the stability to repeated adsorption-desorption cycles, is discussed in reference to their feasibility for industrial use.

2.1 Adsorption equilibrium

The capacity of an adsorbent can be described by the equilibrium sorption isotherm, which is characterised by certain constants whose values express the surface properties and affinity of the adsorbent.

2.1.1 The Langmuir sorption isotherm

This model assumes an ideal, totally homogeneous adsorption surface with a finite number of binding sites and a few interactions between adsorbed molecules (Aksu and Balibek, 2007) is given by:

$$q = \frac{Q_0 b C_e}{1 + b C_e} \quad (1)$$

2.1.2 The Freundlich sorption isotherm

This model is suitable for a highly heterogeneous, energetic distribution of active sites, with interactions between adsorbed molecules (Aksu, 2001; Aksu *et al.*, 2007), and is given by:

$$q = K_F C_e^{1/n} \quad (2)$$

2.1.3 The Redlich-Peterson sorption isotherm

This model is a combination of the Langmuir and Freundlich models and is given by Eq.(3). β lies between 0 and 1. For $\beta = 1$ the Redlich-Peterson model converts to the Langmuir model (Aksu, 2001).

$$q = \frac{K_R C_e}{1 + a_R C_e^\beta} \quad (3)$$

2.1.4 The Fritz-Schluender sorption isotherm

This isotherm for single-component systems more flexible to fit the experimental data since it contains more parameters than any other equilibrium isotherm (Fritz-Schluender, 1974; Yang and Al-Duri, 2005). It is usually written as:

$$q = \frac{K_S C_e^{b_1}}{1 + a_S C_e^{b_2}} \quad (4)$$

2.2 Adsorption kinetics

2.2.1 Kinetic models

Two simplified kinetic equations, from the pseudo first-order and pseudo

second-order kinetic models initially proposed by Lagergren (1989) and Ho and McKay (2000) respectively, were used for a wide range of solute-sorbent systems.

2.2.1.1 Pseudo first-order kinetic model (Lagergren's equation)

This model assumes that the biosorption rate is proportional to the number of unoccupied sites on the biosorption surface (Ozdemir et al., 2003). The kinetic model based on solid capacity gives:

$$q = q_e (1 - e^{-K_1 t}) \quad (5)$$

2.2.1.2 Pseudo second-order kinetic model (Ho's equation)

This model assumes the driving force for adsorption rate comes from the square of the difference between q and q_e . It was transformed to non-linear form, giving as the equation:

$$q = \frac{q_e^2 K_2 t}{1 + q_e K_2 t} \quad (6)$$

2.2.2 Diffusion models

Sorption kinetics is generally controlled by various factors including (i) bulk diffusion, (ii) film diffusion (external mass transfer), (iii) intraparticle diffusion, and (iv) solute adsorption at active sites by the mechanisms of ion exchange, precipitation, complexation or chelation. Different diffusion models propose different diffusion kinetic mechanisms and rate-controlling steps.

2.2.2.1 Intraparticle diffusion model

The model implies that the diffusion from the surface to intraparticle sites is the only rate-limiting step (Yang and Al-Duri, 2005). The model can be expressed as:

$$q = k_p t^{0.5} \quad (7)$$

The half adsorption time $t^{0.5}$ is the time required for the adsorbent to take up half of the adsorbate it has at equilibrium. The rate constant, k_p obtained from the slope of Eq. (11), is related to the intraparticle diffusivity as:

$$k_p = \frac{6q_e}{R} \sqrt{\frac{D}{\pi}} \quad (8)$$

2.2.2.2 Shrinking core model

This model was applied to fluid-particle chemical reactions (Levenspiel, 1972) and, more specifically, to solute adsorption by ion exchange, precipitation, complexation and/or chelation. These processes are controlled by liquid film diffusion, with the extent of the sorption being a function of time given by:

$$X = \frac{3D}{\delta RC} \alpha \quad (9)$$

If the film diffusion is the rate determining process, a plot of X versus α will give a straight line (Preetha and Viruthagirl, 2007). If the process is the particle diffusion control, the model is represented by:

$$F(X) = 1 - 3(1-X)^{\frac{2}{3}} + 2(1-X) = \frac{6D}{R^2 C_0} \alpha \quad (10)$$

Consequently, in this case, a plot of the function $F(X)$ versus α will give a linear relationship, and the diffusivity can be obtained from the slope of such a plot using (Preetha and Viruthagirl, 2007):

$$D = (\text{slope}) \frac{C^0 R^2}{6} \quad (11)$$

2.3 Desorption kinetics

Desorption studies help elucidate the mechanism of adsorption and recover the precious solute, water and adsorbent and also determine the reusability of the beads. As this objective, adsorption-desorption cycles are repeated several times by using the same immobilized biosorbent system. Two simplified kinetic equations, from the pseudo first-order and pseudo second-order kinetic models initially proposed by Lagergren (1989) and Ho and McKay (2000) respectively, are widely used for a wide range of solute-sorbent systems. Ratio of original q/q_e are modified to be equations (12) and (14) of pseudo first-order and pseudo second-order kinetic models, respectively.

$$-\frac{dq}{dt} = k_D q \quad (12)$$

Eq. (12) is integrated under $t = 0$, $q = 0$ until $t = t$, $q = q$ to be Eq.) 13(:

$$\ln\left(\frac{q}{q_e}\right) = -k_D t \quad \text{or} \quad \frac{q}{q_e} = \exp(-k_D t) \quad (13)$$

The desorption kinetic equation of pseudo second-order is modified after integrating to Eq. (14):

$$\frac{q}{q_e} = 1 - \exp(-k_D t) \quad (14)$$

For isothermal diffusion in a spherical adsorbent particle of radius, r , the sorption curve has been shown to follow the following equation (15):

$$\frac{q_t}{q_e} = 1 - \frac{6}{\pi^2} \sum_{n=3}^{\infty} \frac{1}{n^2} \exp\left(-\frac{D}{r^2} n^2 \pi^2 t\right) \quad (15)$$

One of the assumptions of the equation is that the surface concentration of the spherical particle is constant. Hence, this equation was fit using the initial data obtained immediately after the start of desorption experiment, i.e., when the concentration for the regenerating solution remained essentially unchanged. In the short time region, Eq.(16) approaches the limiting parabolic form (Özkaya, 2006):

$$\frac{q}{q_e} = 6 \sqrt{\frac{Dt}{r^2 \pi}} \quad (16)$$

3. Materials and Methods

3.1 Materials

3.1.1 Chemicals

NP was purchased from Fluka Chemical Industries, Ltd. It was a mixture of isomers and used without further purification. Chitosan was a gift from TC Union Company, Thailand. All other chemicals used were of reagent grade.

3.1.2 Microorganisms

Five fungal strains, i.e. *R. arrhizus* TISTR3606, *R. Arrhizus* TISTR3610, *Trichoderma harzianum*, *Aspergillus oryzae* and *Penicillium* sp., available from a microbiological laboratory of Faculty of Liberal Arts and Science, Kasetsart University, were used in this work.

3.1.3 Instruments

Absorbance spectra were recorded on an Ultrospec 3000 UV-Vis spectrometer. Freeze-dried samples were prepared using a Bio-freezer and DW 3 Lyophilyzer (Scientific

promotion Co., Ltd.).

3.2 Methods

3.2.1 Preparation of fungal biomass for NP biosorption.

The five fungal strains were inoculated separately into a growth medium, Tryptone glucose yeast extract (TGY), composed of yeast extract (10 g/L), peptone (20 g/L) and dextrose (20 g/L) in distilled deionised water and cultivated in rotary shaking flasks for 4 days. The biomasses were autoclaved at 121.5⁰C for 15 min and then harvested by filtering through a membrane filter. These were then washed thoroughly with deionised water and freeze-dried. Each sample of dried dead biomass was ground using a mortar and pestle. Particles passing through a 210 µm sieve were used as fungal powder for NP biosorption.

3.2.2 Pre-treatment of biomass

Five-day old living biomass samples, 5 g wet weight, were pre-treated in six different ways: exposure to acid, basic or organic solution, in combination with and without heat treatment as followings: (i) washed and freeze-dried (untreated), (ii) washed and autoclaved for 15 min at 121⁰C, (iii) immersed in a 1 M H₂SO₄ for 1 hour washed and freeze-dried, (iv) immersed in a 2 N NaOH for 1 hour, washed and autoclaved at 121⁰C for 15 min, (v) immersed in a 2 N NaOH and autoclaved at 121⁰C for 15 min, (vi) immersed in a 10% formaldehyde for 1 hour, washed and freeze-dried and (vii) spread on a membrane filter and dried at 50⁰C for 24 hours. The treated fungal biomass was then dried and ground according to the above method 3.2.1. The NP biosorption ability of pre-treated samples was also compared with activated charcoal and commercial chitosan powder.

3.2.3 Biosorption study

Stock solution of nonyphenol (1.00 g/L) was prepared in methanol and stored under dark conditions. Fungal powder (0.02 g, duplicate samples) was added to 20 ml of the 100 mg/L of NP solubilised in 10% methanol in 125 ml conical flasks. The flasks were placed on a rotary shaker (100 rpm, 30⁰C) for 1 hour. Each mixture was filtered through a membrane filter (Whatman No.1), and then extracted with dichloromethane (20 ml) for NP

determination. The concentration of NP in the organic layer was determined by comparing absorbance at a wavelength of 275 nm to a standard curve using dichloromethane as a solvent. The NP uptake was calculated by using:

$$q = \frac{(C_0 - C) * V}{M} \quad (17)$$

In order to optimize the pH for maximum removal efficiency, experiments are conducted in the pH range from 2.0 to 10.0 using 0.02 g of *R. arrhizus* TISTR3610 biomass with 20 ml of 100 mg nonylphenol/L solutions at room temperature. pH of the adsorbate solution is adjusted to set value with 0.01 M HCl and 0.01 M NaOH at the start of the experiment. It is confirmed through the preliminary experiments that the 6 hour is sufficient to attain equilibrium between adsorbent and adsorbate. Each experiment is repeated twice and mean values are taken.

3.2.4 Preparation of the dead beads

The entrapment of *R. arrhizus* TISTR3610 sporangiospores produced immobilised fungal bead biosorbents. Chitosan (2 g) was dissolved in acetic acid solution (3%v/v, 9.9 ml), aseptically heated at 100°C for 5 min, then cooled and mixed with the *R. arrhizus* spore suspension (0.1 ml, about 3.7×10^9 spores/ml). The chitosan suspension was added dropwise to sterilised sodium tri-polyphosphate (2%w/v, 100 ml) and let stand for 3 hours to yield stable 2 mm diameter beads which were washed several times with deionised distilled water. The beads with trapped spores were transferred into TGY medium and incubated on a rotary shaker (100 rpm) at 30°C for 5 days. After this, the chitosan beads with immobilised fungal mycelia were inactivated by autoclaving at 121°C for 15 min, removed from the medium by filtration, washed with distilled water and freeze-dried.

3.2.5 SEM Studies

The cross-section and surface of the fungus immobilised beads were observed by SEM using the preparation method of Pluemsab *et al.* (2007).

3.2.6 Batch kinetic experiments

Kinetic experiments were performed in continuously stirred flasks (100 rpm at 30°C) containing 100 ml NP solution at different concentrations (50-300 mg/L) and 0.1 g of the dead beads. Optimal solution pH was adjusted to 6.5-7.0, since NP is removed more effectively by *R. arrhizus* TISTR 3610 biomass. 2 ml samples were withdrawn at regular intervals and extracted with dichloromethane (2 ml). The organic layer was collected by centrifuging at 3,500 rpm at 4°C. The residual NP concentration was determined by UV/vis spectroscopy at 275 nm (Ultrospec 3000, Pharmacia Biotech Inc., Thailand). This was done for duplicate samples of each treatment.

The validity of the isotherm and kinetic models were checked by plotting Eq. (1)-(11) with the observed data. The kinetic parameters involved in the models were estimated using non-linear regression analysis. By trial and error, and using the *solver* add-in with Microsoft Excel spreadsheet application, the kinetic parameters were determined by minimising the difference between the experimental data and fitted model.

3.2.7 Desorption studies

Desorption studies were conducted in methanol with equilibrium being reached within 90 min. Initially, a known weight of dead beads was placed in 100 mg/L NP solution overnight, and the NP adsorbed determined from the difference between the initial and final NP concentration. The beads were separated from the solution by vacuum filtration.

The NP-beads were mixed with methanol and kept in sealed flasks placed in a shaker at 30°C overnight. The amount of NP desorbed was determined by UV/vis absorbance at 275 nm of wavelength. Various desorption kinetic models were considered and compared against the experimental data for fit. The desorption process was repeated five times to check repeatability.

The desorption ratio was calculated from the amount of NP adsorbed on the biomass and the final NP concentration in desorption medium, that is:

$$\text{Desorption ratio} = \frac{\text{Release nonylphenol (mg)}}{\text{Initially sorbed nonylphenol (mg)}} \times 100 \quad (18)$$

3.2.8 Statistical analyses

The fit of kinetic expressions to the experimental data was tested using the value of coefficient of determination, r^2 (Kumar, 2007), which is defined as:

$$r^2 = \frac{\sum (q_{cal} - \bar{q}_{exp})^2}{\sum (q_{cal} - \bar{q}_{exp})^2 + \sum (q_{cal} - q_{exp})^2} \quad (19)$$

Also used was the non-normalised root mean square (RMS) that weights the actual error at all points (Yang and Al-Duri, 2005), and is defined as:

$$Non-normalized RMS = \sqrt{\frac{\sum_{i=1}^N (q_{cal} - q_{exp})^2}{N}} \quad (20)$$

All statistical data analysis was performed with the help of the toolbox present in Microsoft® Excel (Microsoft Corporation, USA).

4. Results and Discussion

4.1 Screening of fungal biomass for NP biosorption

Five fungal strains, obtained from the culture collection in a laboratory of the Faculty of Liberal Arts and Science, Kasetsart University, were used for the NP biosorption study. Since NP solubility in water is extremely low (5.43 mg/L at 20°C) (Kim *et al.*, 2005), it was extracted from the water layer with dichloromethane before analyses. From an initial concentration of 50 mg/L, the amount of NP absorbed in each fungal mycelia was similar, about 69-76%, as follows: 68.8 ± 2.1% for *R. arrhizus* TISTR3606, 75.9 ± 0.6% for *R. arrhizus* TISTR 3610, 70.6 ± 2.1% for *T. harzatum*, 70.5 ± 0.6% for *A. oryzae*, and 69 ± 4% for *Penicillium* sp. The UV-vis spectra showed decreases in all three main peaks of NP isomer (Fig. 1). The most effective NP absorbent was the mycelia of *R. arrhizus* TISTR 3610, therefore it was selected as a model of the fungal strains for NP biosorption in this work. Also investigated was the use of non-viable and viable *R. arrhizus* biomass to remove phenol and its derivatives from aqueous solutions in batch reactors (Tsezos and Bell, 1989).

4.2 Pre-treatment of fungal biomass and solution pH for NP biosorption

Research has shown that some physical or chemical pre-treatment processes can facilitate more efficient uptake of sorbate as compared to untreated biomass. Six pre-treatments of mycelial biomass of *R. arrhizus* were prepared to observe various chemical and physical effects on both cell walls and intracellular compartments. Heat treatment by autoclave at 121°C for 15 min was found to be the most effective for biosorption with an uptake of 73.7 ± 1.0 mg NP/g (Table 1). Treatments with drying at 50°C for 24 hours or soaking in 10% (v/v) formaldehyde for 1 hour were also fairly effective, with NP uptakes larger than that of untreated biomass at 54 ± 12 mg NP/g. However, the chemical treatments with strong acid or strong base reduced the NP absorption capacity. It could be concluded that the surface modification *in situ* by the pH of these pre-treatments are not appropriate for increased biosorption of this hydrophobic aromatic compound. Therefore, the pre-treatment in the autoclave was selected for the next biosorbent preparation, giving adsorption comparable with the two frequently used commercial biosorbents, activated charcoal (83.1 ± 0.0 mg NP/g) and chitosan (56.3 ± 0.1 mg NP/g) (Table 1).

Table 1 Nonylphenol* biosorption of *Rhizopus arrhizus* TISTR 3610 treated with different mycelial preparations.

Biomass/Biosorbent	NP uptake (mg/g)
<u>Pre-treatment</u>	
Untreated	54.4 ± 11.9
Autoclaved (121°C, 15 min)	73.7 ± 1.0
1M H ₂ SO ₄ for 1 hour	49.8 ± 5.1
1N NaOH for 1 hour	37.1 ± 0.0
1N NaOH at 121°C for 15 min	4.5 ± 3.4
10% (v/v) formaldehyde for 1 hour	68.3 ± 0.4
Dried at 50°C for 24 hours	61.2 ± 7.9
<u>Commercial biosorbents</u>	

Activated charcoal	83.1 ± 0.0
Chitosan	56.3 ± 0.1

* Initial NP concentration of 100 mg/L, performed at 100 rpm, at 30°C for 1 hour.

Biosorption of NP exhibited an uptake capacity over 78% and 85% with wide initial pH ranges of 3.1-10.0 and 5.7-7.5, respectively. Maximal NP removal of 87% was obtained at an initial pH 6.6. At initial pH 2.3, however, the NP uptake decreased to 62%. pH solutions at equilibrium under specified conditions in this work were found approximately to decrease from 5.7-7.5 to 4.0-4.9. Accordingly, NP are considered to be molecular form in the range of pH \leq 7.0 (its pKa = 10.28) (Fan *et al.*, 2008). Therefore, NP effectively adsorbed onto fungal biomass in the form of molecules rather than phenolate anion derivatives. The molecular interactions, i.e. hydrogen bonding, hydrophobic interaction and Van der Waals forces could play an important role for the NP adsorption. Neither positive nor negative charges resulting from the biosorbent and pH solution is attractive through electrostatic force for NP biosorption. Nadavala *et al.* (2009) described both phenol and o-chlorophenol existing predominantly as neutral species at pH 7.0. Their interaction with the chitosan-calcium alginate blended beads is considered mainly as non-polar, and the forces responsible for adsorption are physical van der Waals forces.

4.3 Properties of the dead beads

There are a number of immobilisation methods using dead grinded fungal biomass encapsulated in polymer matrix, including calcium alginate and polyvinyl alcohol (Wu and Yu, 2007). In the present study, asexual spores of *R. arrhizus* were trapped into chitosan beads by a liquid curing method in the presence of TPP, and then cultivated for 5 days for complete spore germination. After this period, the hyphae would convert to a sporulation cycle. The bead surface was found to have homogeneously distributed exuberant mycelia inside, and outward growing mycelia covering the whole particle surface (Fig. 2). The dry weight of immobilised fungus in the support was 9.7×10^{-4} g/bead. The dried chitosan-immobilised fungal beads had a diameter of approximately 4 mm with a

spherical shape which was completely different from the 1-1.5 mm diameter dried plain beads. It also improves the affinity of the biosorbent for the solute by providing directly exposure without any barriers. The dead beads were also stronger and more stable than plain chitosan beads when immersed in acid solution (data not shown), even at pH = 1.

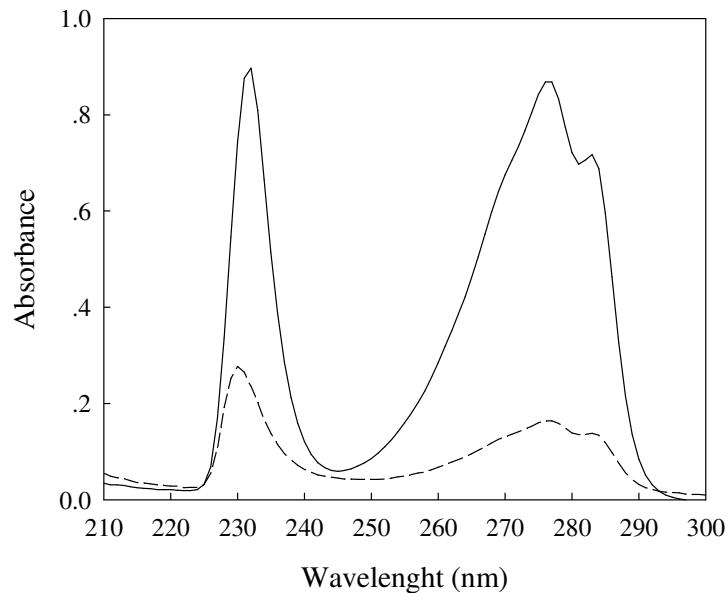


Fig. 1 Typical UV-VIS spectrum of NP before (—) and after (---) treatment with fungal grill for 1 hour.



Fig. 2 SEM photograph of the cross section of chitosan immobilised bead.

4.4 Evaluation of adsorption isotherms

To model NP biosorption and gain a better understanding of the sorption process, the four adsorption isotherms, Eq.(1-4) were compared to the experimental data for fit. The adsorption isotherm constants with the corresponding correlation coefficients, Eq.(19) and non-normalised RMS, Eq.(20) for each model are presented in Table 2. Although linear regression has been the most commonly used method to obtain the parameters and determine the fit of the kinetic expressions, non-linear regression provides a better measure of fit (Kumar, 2007). As compared to non-linear analysis, the correlation coefficients (r^2) of 0.8912 (Redlich-Peterson), 0.9320 (Freundlich) and 0.7561 (Langmuir), except that for the non-linearized Fritz-Schlüender, were obtained from the fitting parameters by linear regression. From the results shown in Table 2, the four-parameter isotherm models of Fritz-Schlüender gave the best fit with $r^2 = 0.9984$, followed by the three- and two-parameter isotherm models of Redlich-Peterson ($r^2 = 0.9302$), Freundlich ($r^2 = 0.9287$) and Langmuir ($r^2 = 0.9271$). Yang and Al-Duri (2005) also observed the superiority of the Fritz-Schlüender model over the other models for biosorption of three reactive dyes onto activated carbon. Based on the Freundlich isotherm plot, the adsorption capacity (K_F) was found to be 30.25 mg/g with an adsorption intensity (n) of 1.87. These were similar values to those for the biosorption of pentachlorophenol onto live *R. arrhizus* which has a K_F of 32.13 mg/g and n of 1.79 (Tsezos and Bell, 1989). The high value of the maximum adsorption capacity, Q_0 of 312.17 mg/g and the low value of the Langmuir constant, b of 0.05 L/mg were obtained with the Langmuir isotherm. In general, a small value of b indicates that the adsorbate has a high binding affinity for the biosorbent (Arica *et al.*, 2003). A similar observation was reported for 2,4-dichlorophenol biosorption onto free and calcium alginate immobilised biomass of white-rot fungus *Phanerochaete chrysosporium* with b values of 0.039 and 0.053 L/mg, respectively (Wu and Yu, 2007). The values of K_F and Q_0 also indicate the great affinity for NP by the beads in this study.

Table 2 Parameters from fitting the adsorption equilibrium data to various isotherm models

Langmuir constants	
Q_0 (mg/g)	312.17
b (L/mg)	0.05
R^2	0.9271
Non-normalised RMS	20.4009
Freundlich constants	
K_F	30.25
N	1.87
R^2	0.9287
Non-normalised RMS	18.5402
Redlich-Peterson constants	
K_R	180.94
α_P	5.26
β	0.49
R^2	0.9302
Non-normalised RMS	18.4794
Fritz-Schluender constants	
K_s	46.87
a_s	0.67
B_1	0.74
B_2	0.35
K_s/a_s	70.47
R^2	0.9984
Non-normalised RMS	18.4617

Note: Parameters determined using non-linear regression in Microsoft® Excel (Microsoft Corporation, USA).

4.5 Evaluation of adsorption kinetics

The rate constants for the pseudo first-order (K_1) and pseudo second-order (K_2) sorption reactions were obtained by plotting the non-linear curves fitting Eq.(5) and (6). Kinetic rate constants for NP uptake by the dead beads are presented in Table 3. From the correlation coefficients, the experimental adsorption data gave a better fit to pseudo first-order in the concentration range of 58.62-189.91 mg/L. The corresponding kinetic models are plotted in Fig 3. Using Eq.(7), the plots of intraparticle diffusion with NP uptake versus t at different initial NP concentrations (20.12-245.15 mg/L) are shown in Fig 4. The plots were not linear over the whole time range, implying that more than one process affected the adsorption. Three linear regions better describe the intraparticle diffusion when the initial concentration of NP was in the range 58.62-245.15 mg/L. The initial linear sections have steeper slopes than the subsequent sections. The multi-linearity of the plots can be compared to the three steps of acid dye adsorption onto chitosan reported by Cheung *et al.* (2007). The first, steeper section was attributed to the diffusion of solute through the solution to the external surface of the adsorbent, or the boundary layer diffusion of solute molecules. The second section was attributed to the gradual adsorption stage with diffusion into the mesopores, where intraparticle diffusion was the rate limiting process. The third portion was attributed to the final equilibrium stage for which the intraparticle diffusion started to slow due to the extremely low solute concentration remaining in the solution, and relates to adsorption of the solute into micropores. The slopes of the linear sections indicate the rates of adsorption, a shallower slope corresponding to a slower adsorption process. Thus, it can be implied that the rate-controlling step of NP adsorption was essentially intraparticle diffusion. In addition, relatively low to moderate levels of initial NP concentration (20.12-189.91 mg/L) induced adsorption into micropores as observed from the nearly parallel third section of the plots. The intraparticle diffusivity (D) and intraparticle diffusion rate constant (k_p) significantly increase with increased initial NP concentration (Table 4). On the other hand, using a shrinking core model and plotting $F(X)$ against α shows significant linear relationships (Fig. 5b), as compared to plotting X against α (Fig. 5a). The diffusivity values are in the range of 2.37×10^{-4} to 1.89×10^{-4} $\text{cm}^2 \text{s}^{-1}$. Clearly, this implies that

intraparticle diffusion is the rate controlling step for the NP biosorption in this work. Although intraparticle diffusion and shrinking core models can describe the biosorption process for NP uptake by the dead beads reasonably well, an initial NP concentration was quite limited lower than approximately 200 mg/g (Fig. 5).

Table 3 Kinetic parameters for pseudo first-order and pseudo second-order biosorption and desorption of NP using dead beads.

	Nonylphenol		Pseudo first-order rate				Pseudo second-order rate			
	C_0	q	K_1	q_e	r^2	Non-normalized RMS	K_2	q_e	r^2	Non-normalized RMS
	(mg/l)	(mg/g)	(min ⁻¹)	(mg/g)			(g/mg min)	(mg/g)		
Biosorption			0.10227		0.6726	2.0072	1.03×10^{-2}		0.5742	2.2347
	20.1156	19.4558		16.4679				17.2494		
			0.03606		0.9878	1.7437	7.41×10^{-4}		0.9921	1.3298
	58.6191	55.9184		54.3062				61.3428		
	115.3538	100.5443	0.02267	102.5006	0.9107	10.2708	1.91×10^{-4}	122.9755	0.8635	12.7894
	189.9116	171.9728	0.02705	171.2495	0.9150	16.1795	1.47×10^{-4}	200.9999	0.8753	21.0549
	245.1497	207.4150	0.01119	224.9302	0.8597	30.8957	1.76×10^{-5}	338.0162	0.6926	50.3715
Desorption	-	145.6420	0.40945	138.1793	0.5655	29.5331	4.98×10^{-3}	145.8314	0.9997	5.2708

Note: Parameters determined using non-linear regression in Microsoft® Excel (Microsoft Corporation, USA).

Table 4 Intraparticle diffusion and shrinking core coefficients

Initial concentration of NP (mg/L)	Intraparticle diffusion			Shrinking core model		
	Slope	k_p mg/(g. min ^{0.5})	Diffusion coefficient (cm ² /s)	Slope	C^0 (mg/L)	Diffusion coefficient (cm ² /s)
20.12	1.21	9.79×10^1	0.15	1.89×10^{-3}	1.03	2.37×10^{-4}
58.62	3.76	9.32×10^2	1.67	5.89×10^{-4}	2.95	2.80×10^{-4}
115.35	8.38	3.30×10^3	6.50	4.41×10^{-4}	5.30	3.65×10^{-4}
189.91	12.30	8.80×10^3	15.75	2.21×10^{-4}	9.07	2.98×10^{-4}
245.15	14.70	1.31×10^4	24.01	1.22×10^{-4}	10.94	1.89×10^{-4}

Bead dosage = 0.1 g, NP solution volume = 100 ml, bead amount = 18 beads

Note: Parameters determined using non-linear regression in Microsoft® Excel (Microsoft Corporation, USA)

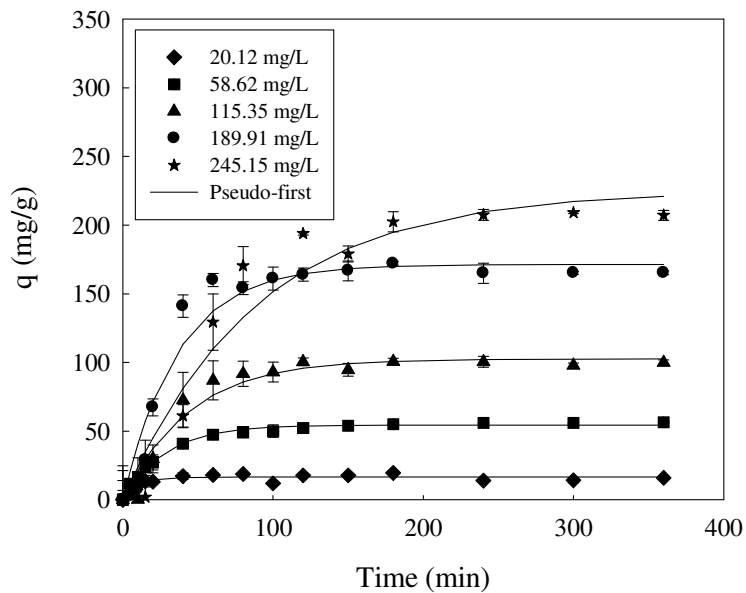


Fig. 3 Adsorption kinetics of nonylphenol by the dead beads described with the pseudo first-order model Eq.(5).

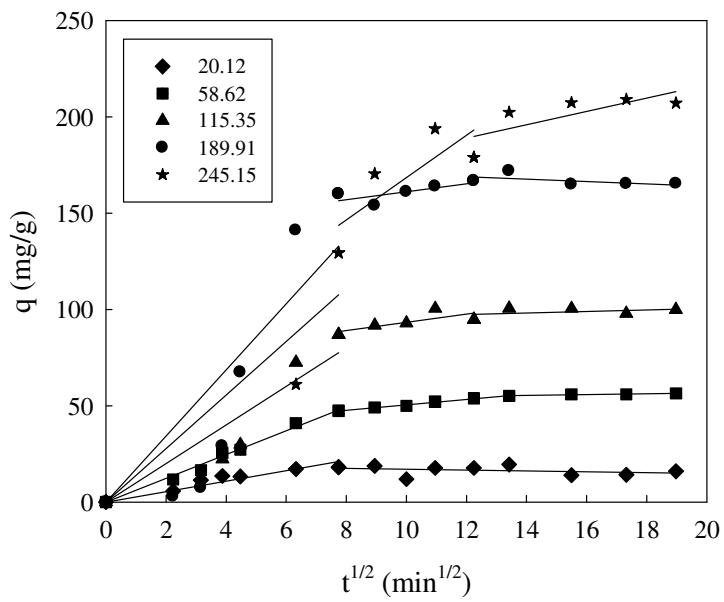


Fig. 4 Intraparticle diffusion kinetics for nonyphenol biosorption on the dead beads (multi-linearity) described with Eq.(7).

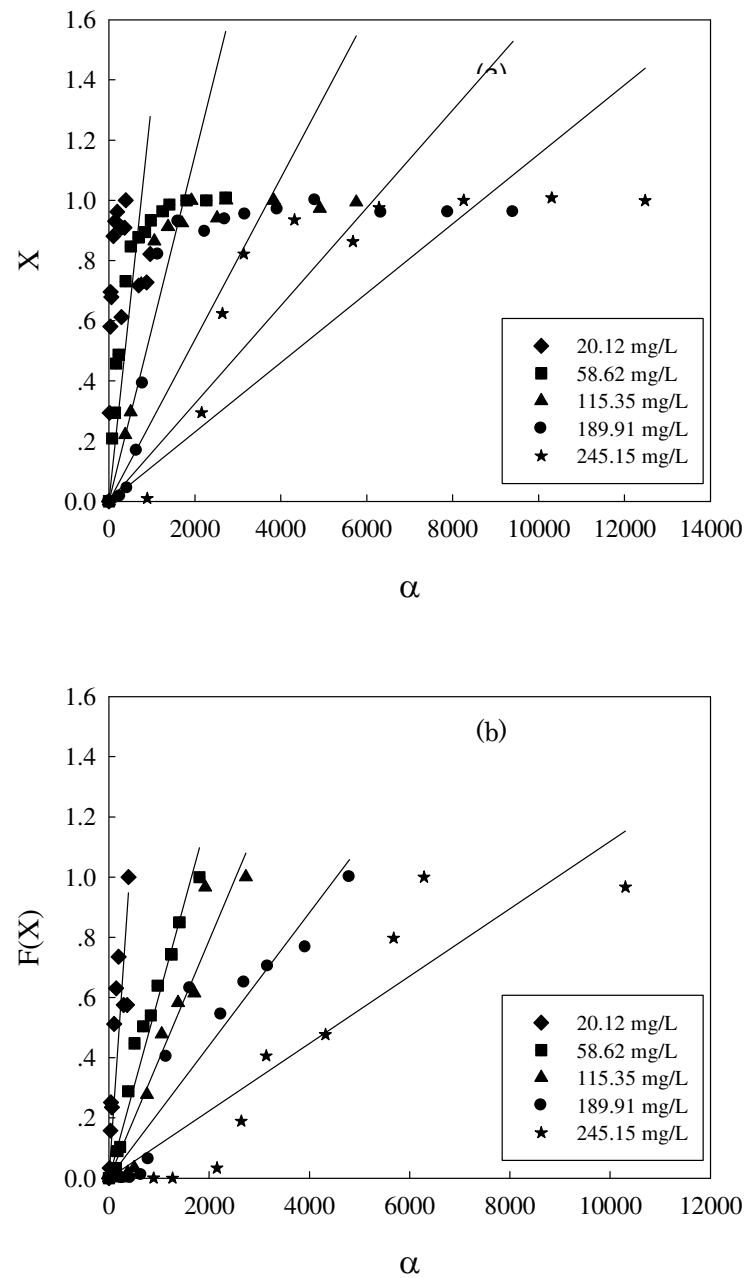


Fig. 5 Shrinking core model for (a) external film diffusion control and (b) particle diffusion control.

4.6 Desorption kinetics

Desorption studies elucidate the mechanism of adsorption and recovery of NP from water, its interaction with the adsorbent. The adsorbed NP remains mostly stable on the adsorbent and can be desorbed using methanol. It can be seen that the desorption process of NP can well described by a pseudo second-order model using a non-linear regression method (Fig. 6). This was evident from the high r^2 value of 0.9997 and low non-normalised RMS value of 5.2708 as shown in Table 3. NP desorption by methanol also occurred rapidly ($K_2 = 4.98 \times 10^{-3}$ g/mg min). Although, it has been reported that distilled water (Wu and Yu, 2007), CaCl_2 solution (Benoit *et al.*, 1998) and NaNO_3 solution (Daughney and Fein, 1998) can be used to desorb solutes from phenol-loaded and chlorophenol-loaded biomass, using methanol as the desorbing agent allows for easy regeneration as it can be separated from nonylphenol by vapourisation. The NP waste can then be further degraded by chemical or physical treatments (Maniero *et al.*, 2008). The regenerated dead beads are also reusable and, from this study, active in four batches (Fig. 7). The weight loss of dead beads was 43% by the end of the fifth batch use.

Table 5 Desorption kinetics for pseudo first-order and pseudo second-order of NP using dead beads by non-linear regression method at 25 min.

Parameters	pseudo first-order	pseudo second-order	pore diffusion*
q_e (mg/g)	105.5145	105.9194	-
K_D	0.0212	-0.2243	-
D/R^2 (min ⁻¹)	-	-	1.0929×10^{-6}
r^2	0.3807	0.7957	0.6673
RMS	0.3385	0.1034	0.1479

* $r = 0.12$ cm.

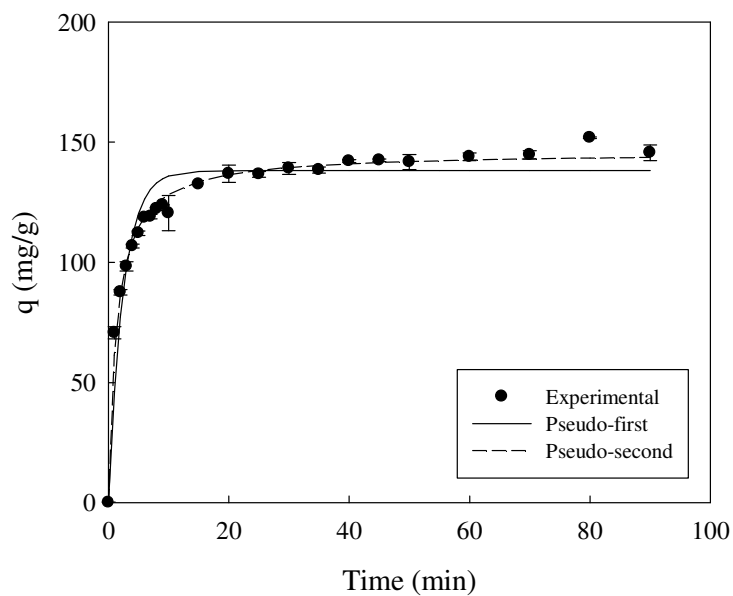


Fig. 6 Comparison of two desorption kinetic models for NP removal by the dead beads.
Curve fitting performed with SigmaPlot 11.0 (Systat Software Inc., USA).

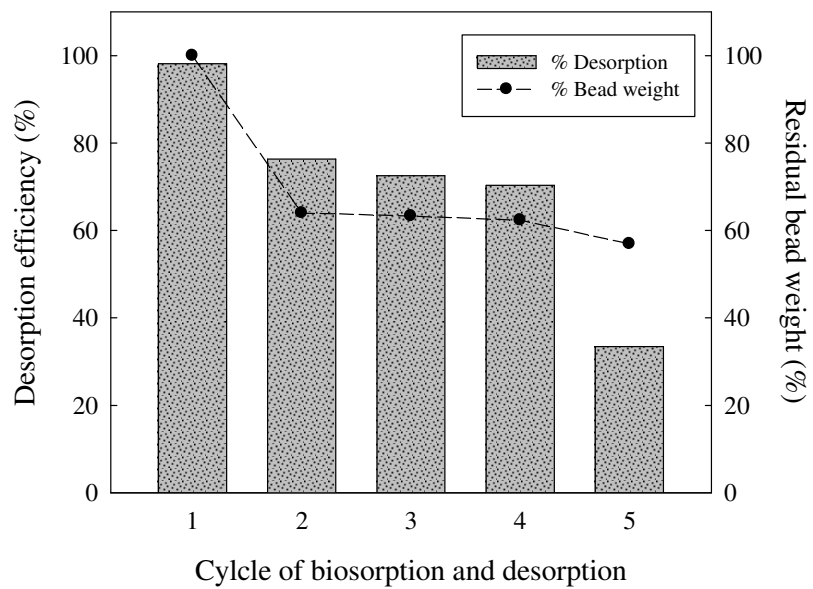


Fig. 7 Desorption efficiency of the dead beads after repeated NP biosorption and NP desorption with methanol.

4.7 Selectivity of the beads on nonylphenol biosorption

The adsorption selectivity of the beads for NP was excellently higher than the two similar structure compounds, phenol and polyethyleneglycol(4-nonylphenol-3-sulfopropyl ether, potassium salt (PSE) (Fig. 8). Desorption to recover the adsorbed NP from the beads was performed in methanol and was best described using a pseudo second-order kinetic model compared to pore diffusion model and pseudo first-order. The second-order desorption rate (K_{D2}) constant was determined as 0.2243 g/mg min. The regeneration of used dead beads was effective for at least 3 batch consecutive cycles which almost NP uptake could still be eluted.

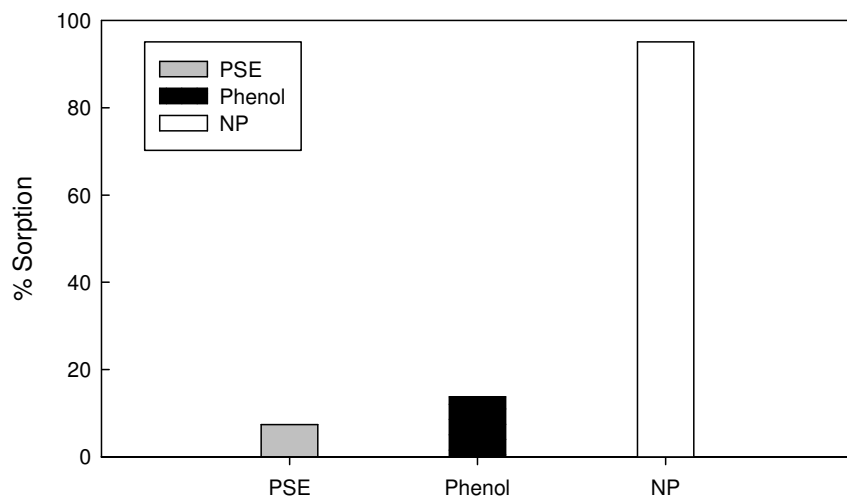


Fig 8. Adsorption selectivity of the beads for NP, phenol, and polyethylene glycol (4-nonylphenol-3-sulfopropyl ether, potassium salt (PSE).

5. Conclusion

The use of chitosan-immobilised beads was effective for an innovative treatment of low soluble recalcitrant pollutant from wastewater. The fungal dead biomass could be prepared readily on a commercial scale as an alternative low-cost biosorbent for use in wastewater treatment plants. In this work, the dead beads were pretreated with moist heat which substantially increased their capacity of NP biosorption. Equilibrated NP adsorption

with the dead beads best fitted the Fritz-Schlünder isotherm. A maximal monolayer capacity of the dead beads was over 312 mg/g. The rate of NP biosorption was rapid in the first 40 min of contact time. The kinetics for adsorption of NP onto the dead beads was well described by the pseudo first-order equation, while that for desorption was well described by the pseudo second-order one. Both intraparticle diffusion and shrinking core models were found suitably consistent with the adsorption experimental data, especially at the NP concentration less than 200 mg/L. The regeneration of used dead beads with methanol was effective for at least 4 batch cycles in this study. As mentioned, the production of the dead beads and their possible reuses provides an alternative biosorbent for NP removal, as well as for other hydrophobic aromatic recalcitrant pollutants in wastewater.

6. References

Ahel, M., McEvoy, J., Giger, W. 1993. Bioaccumulation of the lipophilic metabolites of nonionic surfactants in freshwater organisms. *Environ. Pollut.* 79, 243-248.

Aksu, Z. 2001. Biosorption of reactive dyes by dried activated sludge: equilibrium and kinetic modeling. *Biochem. Eng. J.* 7, 79-84.

Aksu, Z. 2005. Application of biosorption for the removal of organic pollutants: a review. *Process Biochem.* 40, 997-1026.

Aksu, Z., Balibek, E. 2007. Chromium (VI) biosorption by dried *Rhizopus arrhizus*: Effect of salt (NaCl) concentration on equilibrium and kinetic parameters. *J. Hazard. Mat.* 145, 210-220.

Asku, Z., Cagatay, S.S., Gönen, F. 2007. Continuous fixed bed biosorption of reactive dyes by *Rhizopus arrhizus*: Determination of column capacity. *J. Hazard. Mat.* 143, 362-371.

Arica, M.Y., Arpa, Ç., Ergene, A., Bayramoğlu, G., Genç, Ö. 2003. Ca-alginate as a supper for Pb(II) and Zn(II) biosorption with immobilized *Phanerochaete chrysosporium*. *Carbohyd. Polym.* 52, 167-174.

Benoit, P., Barriuso, E., Calvet, R. 1998. Biosorption characterization of herbicides, 2,4-D

and atrazine, and two chlorophenols on fungal mycelium. *Chemosphere* 37, 1271-1282.

Cheung, W.H., Szeto, Y.S., Mckay, G. 2007. Intraparticle diffusion processes during acid dye adsorption onto chitosan. *Bioresour. Technol.* 98, 2897-2904.

Daughney, C.J., Fein, J.B. 1998. Sorption of 2,4,6-trichlorophenol by *Bacillus subtilis*. *Environ. Sci. Technol.* 32, 749-752.

Ekelund, R., Bergman, A., Granmo, A., Berggren, M. 1990. Bioaccumulation of 4-nonylphenol in marine animals. A re-evaluation. *Environ. Pollut.* 64, 107-120.

Fritz, W., Schluender, E.V. 1974. Simultaneous adsorption equilibria of organic solutes in dilute aqueous solutions on activated carbon. *Chem. Eng. Sci.* 29, 1279-1282.

Fan, J., Fan, Y., Pei, Y., Wu, K., Wang, J., Fan, M. 2008. Solvent extraction of selected endocrine-disrupting phenols using ionic liquids. *Sep. Puri. Technol.* 61, 324-331.

Fu, Y., Viraraghavan, T. 2001. Fungal decolorization of dye wastewaters: a review. *Bioresour. Tech.* 79, 251-262.

Granmo, A., Ekelund, R., Magnusson, K., Berggren, M. 1989. Lethal and sublethal toxicity of 4-nonylphenol to the common mussel. *Environ. Pollut.* 59, 115-127.

Helander, I.M., Nurmiaho-Lassila, E.L., Ahvenainen, R., Rhoades, J., Roller, S. 2001. Chitosan disrupts the barrier properties of the outer membrane of gram-negative bacteria. *Inter. J. Food Microbiol.* 71, 235-244.

Ho, Y.S., Mckay, G. 1999. Pseudo second-order model for sorption processes. *Process Biochem.* 34, 451-465.

Ho, Y.S., Mckay, G. 2000. The kinetics of sorption of divalent metal ions onto sphagnum moss peat. *Water Res.* 34, 735-742.

Kapoor, A., Viraraghavan, T. 1995. Fungal biosorption-an alternative treatment option for heavy metal bearing wastewaters: a review. *Bioresour. Technol.* 53, 195-206.

Kapoor, A., Viraraghavan, T. 1998. Removal of heavy metals from aqueous solutions using immobilized fungal biomass in continuous mode. *Water Res.* 32, 1968-1977.

Kawasaki, N., Araki, M., Nakamura, T., Tanada, S. 2001. Inclusion behavior of 4-nonylphenol

into cyclodextrin derivatives. *J. Colloid Inter. Sci.* 238, 215–218.

Kim, J., Korshin, G.V., Velichenko, A.B. 2005. Comparative study of electrochemical degradation and ozonation of nonylphenol. *Water Res.* 39, 2527-2534.

Kumar, K.V. 2007. Pseudo second-order models for the adsorption of safranin onto activated carbon: Comparison of linear and non-linear regression methods. *J. Hazard. Mat.* 142, 564-567.

Lagergren, S. 1989. About the theory of so-called adsorption of soluble substances. *Kungliga Svenska Vetenskapsakademiens Handlingar*, Band 24, 1-39.

Lavenspiel, O. 1972. Chemical Reaction Engineering. John Wiley & Sons. 2nd ed., 21-32, 69-71, 357-408.

Maniero, M.G., Bila, D.M., Dezotti, M. 2008. Degradation and estrogenic activity removal of 17 β -estradiol and 17 α -ethinylestradiol by ozonation and O₃/H₂O₂. *Sci. Total Environ.* 407, 105-115.

Nakada, N., Tanishima, T., Shinohara, H., Kiri, K., Takada, H. 2006. Pharmaceutical chemicals and endocrine disrupters in municipal wastewater in Tokyo and their removal during activated sludge treatment. *Water Res.* 40, 3297-3303.

Nadavala, K.S., Swayampakula, K., Boddu, M.V., Abburi, K. 2009. Biosorption of phenol and o-chlorophenol from aqueous solutions on to chitosan–calcium alginate blended beads. *J. Hazard. Mat.* 162, 482–489.

Nevskaia, D.M., Guerrero-Ruiz, A. 2001. Comparative study of the adsorption from aqueous solutions and the desorption of phenol and nonylphenol substrates on activated carbons. *J. Colloid Inter. Sci.* 234, 316-321.

Özkaya, B. 2006. Adsorption and desorption of phenol on activated carbon and a comparison of isotherm models. *J. Hazard. Mat.* B129, 158-163.

Pluemsab, W., Fukazawa, Y., Furuike, T., Nodasaka, Y., Sakairi, N. 2007. Cyclodextrin-linked alginate beads as supporting materials for *Sphingomonas cloacae*, a nonylphenol degrading bacteria. *Bioresour. Technol.* 98, 2076-2081.

Preetha, B., Viruthagirl, T. 2007. Batch and continuous biosorption of chromium (VI) by

Rhizopus arrhizus. Sep. Puri. Technol. 57, 126-133.

Singh, A., Kumar, D., Gaur, J.P. 2008. Removal of Cu(II) and Pb(II) by *Pithophora oedogonia*: Sorption, desorption and repeated use of the biomass. J. Hazard. Mat. 152, 1011-1019.

Tsezos, M., Bell, J.P. 1989. Comparison of the biosorption and desorption of hazardous organic pollutants by live and dead biomass. Water Res. 23, 561-568.

Wu, J., Yu, H.Q. 2007. Biosorption of 2,4-dichlorophenol by immobilized white-rot fungus *Phanerochaete chrysosporium* from aqueous solutions. Bioresour. Technol. 98(2), 253-259.

Yang, X.Y., Al-Duri, B. 2005. Kinetic modeling of liquid-phase adsorption of reactive dyes on activated carbon. J. Colloid Inter. Sci. 287, 25-34.

7. Acknowledgements

This work was supported by Thailand Research Fund (TRF) under the research grants “MRG5080420” and “RPUS-I251A13001” awarded in 2007 and 2008, respectively. The authors are grateful to the Faculty of Liberal Arts and Science and the Faculty of Agro-Industry, Kasetsart University, for facilitating the research, and additional Wilhelm J. Holzschuh of the Faculty for proof reading the manuscript.

Output จากโครงการวิจัยที่ได้รับทุนจาก สกอ.

1. ผลงานวิจัยตีพิมพ์ในวารสารวิชาการนานาชาติ

- Lang W., Dechma C., Sirisansaneeyakul S., and Sakairi N. Biosorption of nonylphenol on dead biomass of *Rhizopus arrhizus* encapsulated in chitosan beads. *Bioresource Technology*. 2009 (In press). มี impact factor 3.103

2. การนำผลงานวิจัยไปใช้ประโยชน์

เชิงวิชาการ

- เพื่อเป็นแนวทางในการบำบัดน้ำเสียจากโรงงานทอผ้าหรือโรงงานที่ใช้สี้อมโดยมีการพัฒนาเทคนิคการผลิตวัสดุดูดซับทางชีวภาพโดยใช้ไคโตซานซึ่งผลิตมาจากวัสดุเหลือใช้และมีราคาถูก
- พัฒนาเทคนิคการใช้ไคโตซานเป็นวัสดุตึงเชือราชี่งโดยทั่วไปไคโตซานมักไม่สามารถใช้ตึงเซลล์จุลทรรศน์ได้เนื่องจากมีฤทธิ์เป็นสารผ่าเชือแบบที่เรียบและฟังไจอันเกิดจากคุณสมบัติการเกาะจับกับผนังเซลล์
- สร้างองค์ความรู้ใหม่ในเรื่องการดูดซับสารอนินิลฟีนอลซึ่งเป็นกลุ่มสารยับยั้งการทำงานของต่อไร้ท่อด้วยเม็ดราไร์ชีวิตที่ตึงด้วยไคโตซาน

3. อื่น ๆ

ผลงานวิจัยตีพิมพ์ระดับชาติ

1. วีรานุช หลาง, ชมารณ เดชมา, วันวิสาข์ บูรณบริภัณฑ์, สาโรจน์ ศิริศันสนียกุล. แบบจำลองทางจนผลศาสตร์ของการดูดซับและการคายสารอนินิลฟีนอลด้วยเส้นใยราไร์ชีวิตที่เจริญและถูกตึงในเม็ดไคโตซาน. วารสารสิ่งแวดล้อมและทรัพยากรธรรมชาติ. 2009 (accepted).

การประชุมวิชาการระดับชาติ

1. ชมารณ เดชมา, ดวงพร สาระทองคุณ, พิชญ์พงศ์ บัวแก้ว, วันวิสาข์ บูรณบริภัณฑ์, วีรานุช หลาง. การพัฒนาเทคนิคการผลิตเม็ดราไร์ชีวิตที่ตึงด้วยไคโตซานเพื่อใช้เป็นวัสดุดูดซับสารอนินิลฟีนอล. งานแสดงนิทรรศการโครงการอุดสาหกรรมสำหรับนักศึกษาระดับปริญญาตรี ครั้งที่ 7. 26-29

มีนาคม 2009. สยามพารากอน, กรุงเทพฯ. เลขที่โครงการ R51A13001.

2. วีระนุช หลาง, ชุมวรรณ เดชมา, ดวงพร สรัsthongken, สาโรจน์ ศิริศันสนีย์
กุล, Nobuo Sakairi, การดูดซับน้ำฝนโดยใช้มวลชีวภาพฟังไจตรีงที่เร็ว
ชีวิต. การประชุมวิชาการ สกอ. ครั้งที่ 8. 16-18 ตุลาคม 2008. โรงแรมออลิ
เดย์ อินน์ รีสอร์ทรีเจนท์ บีช เพชรบุรี.



2 Biosorption of nonylphenol on dead biomass of *Rhizopus arrhizus* 3 encapsulated in chitosan beads

4 Weeranuch Lang^{a,*}, Chomawan Dejma^a, Sarote Sirisansaneeyakul^b, Nobuo Sakairi^c

5 ^a Department of Microbiology, Faculty of Liberal Arts and Science, Kasetsart University, Kampaeng Saen, Nakorn-Pathom 73140, Thailand

6 ^b Department of Biotechnology, Faculty of Agro-Industry, Kasetsart *University*, 10900, Thailand

7 ^c Graduate School of Environmental Science, Hokkaido University, Kita-ku, Sapporo 060-0810, Japan

8 ARTICLE INFO

11 Article history:

12 Received 20 February 2009

13 Received in revised form 2 June 2009

14 Accepted 7 June 2009

15 Available online xxxx

16 Keywords:

17 Biosorption

18 Nonylphenol

19 *Rhizopus arrhizus*

20 Chitosan

21 Kinetic modelling

22 ABSTRACT

The nonylphenol (NP) biosorption and desorption potential for fungal biomass used under batch conditions was investigated using kinetics and isotherm models. Fungal biomass of *Rhizopus arrhizus* TISTR 3610 exhibited preferential uptake of NP, an endocrine disrupting chemicals. Sporangiospores, asexual spores, were immobilisation in chitosan beads. The biosorption data of NP on the moist heat inactivated *R. arrhizus*-chitosan beads were analyzed using four popular adsorption isotherms and, by using non-linear least-regression with the solver add-in in Microsoft Excel, correlated in order with the *Fritz-Schlünder* > *Redlich-Peterson* > Freundlich > Langmuir isotherms. The pseudo first-order kinetics was found to have the best fit with the experimental data. The diffusivity of NP in the *R. arrhizus*-chitosan beads was calculated using the shrinking core model, and the diffusivity values were in the ranges of 2.3736×10^{-4} – 1.8950×10^{-4} cm² s⁻¹. Desorption to recover the adsorbed NP from the beads was performed in methanol and was best described using a pseudo second-order kinetic model.

© 2009 Published by Elsevier Ltd.

37 1. Introduction

39 Nonylphenol (NP) is one of the organic pollutants found in
40 aquatic environments as a consequence of the biodegradation of
41 nonylphenol polyethoxylate (NPnEO), a non-ionic surfactant con-
42 tained in industrial cleaning products and in household detergents
43 (Ahel et al., 1993). Although the parent surfactant itself is less
44 toxic, NPnEO released into the environment rapidly decomposes
45 to form NP which is the most recalcitrant intermediate of NPnEO
46 decomposition. Principally NP persists in sewage treatment plants
47 and outflows (Nakada et al., 2006), and tends to accumulate in the
48 fatty tissue of aquatic organisms when released into aquatic
49 environments.

50 NP is known to be an endocrine disruptor compound, that is,
51 it mimics endogenous hormones and disrupts important life pro-
52 cesses. Substantial evidence exists to demonstrate that NP causes
53 various disorders of the male reproductive system, including re-
54duced testicular size and lower sperm production in rainbow
55 trout and other marine animals (Granmo et al., 1989; Ekelund
56 et al., 1990). NP and NPnEO have been banned in the European
57 Union as a hazard to human and environmental safety. However,
58 NP and NPnEO are still widely used in Thailand and other Asian
59 countries, especially as industrial detergents such as those used
60 for wool washing and metal finishing, in various laboratory

61 detergents including Titron X-100, in industrial processes such
62 as emulsion polymerisation, and in some pesticide formulations.

63 Although the techniques of adsorption on activated carbon,
64 photo-oxidation and ozone treatment for NP removal have been
65 studied and found to be effective, cost-effectiveness is the main
66 limitation against widespread practical use (Nevskaya and Guer-
67 ruo-Ruiz, 2001; Kawasaki et al., 2001). The search for a low cost
68 and easily available adsorbent has led the authors to investigate
69 materials of agricultural and biological origin, and some indus-
70 trial by-products as adsorbents.

71 Biosorption, the passive uptake of pollutants by non-growing
72 or non-living microbial biomass such as bacteria, fungi and al-
73 gae, is considered to have good potential for the removal of
74 non-degradable pollutants from aqueous solution (Kapoor and
75 Viraraghavan, 1995). Reports of biosorption of toxic organic com-
76 pounds with biomass showed that better removal was obtained
77 with dead biomass than with live biomass (Aksu, 2005). Immo-
78 bilisation may also allow higher biomass concentrations, and
79 facilitate separation and non-destructive recovery of biomass
80 from pollutant-bearing solution (Fu and Viraraghavan, 2001).
81 Immobilised fungal biomass has been used for the removal of
82 various metals, dyes and some organic pollutants (Kapoor and
83 Viraraghavan, 1995; Aksu, 2005) but no study has been con-
84 ducted on the use of immobilised biomass for the removal of
85 NP or other endocrine disruptor compounds. Therefore, there is
86 a need to study the performance of the immobilised fungus sys-
87 tem with NP.

* Corresponding author. Tel.: +66 34 281 105 7; fax: +66 34 281 057.
E-mail address: faaswnp@ku.ac.th (W. Lang).

Nomenclature

V	volume of aqueous phase (L)
M	mass of biomass (g)
a_S	Fritz–Schlünder isotherm constant (mg/L) $^{-b_2}$
a_R	Redlich–Peterson isotherm constant (L/mg) $^\beta$
b	Langmuir isotherm constant (L/mg)
b_1, b_2	Fritz–Schlünder isotherm constants (dimensionless)
C	concentration of NP at time, t (ppm)
C_0	initial concentration of NP (ppm)
C^0	$\frac{(C_0 - C_e)V}{n^3 \pi R^3}$, average NP binding site density (ppm)
C_e	concentration of NP at equilibrium (ppm)
D	diffusion coefficient (cm 2 /s)
K_1	pseudo first-order rate constant (min $^{-1}$)
K_2	pseudo second-order rate constant modified (g/mg min)
k_p	intraparticle diffusion rate constant (mg/g min $^{0.5}$)
K_F	Freundlich constant, characteristic of the system related to the adsorption capacity (mg/g)
K_R	Redlich–Peterson isotherm constant (L/g)
K_S	Fritz–Schlünder isotherm constant (mg/g) (mg/L) $^{-b_1}$
n	Freundlich constant, characteristic of the system related to the adsorption intensity (dimensionless)
q	NP uptake rate (mg/g)

q_e	NP uptake rate at equilibrium (mg/g)
Q_0	Langmuir adsorption isotherm constant (mg/g) (dependent on the maximum adsorption capacity of biosorbent)
R	radius of bead (cm)
t	contact time (min)
$X, F(X)$	functions derived from the shrinking core model (Preetha and Viruthagirl, 2007)
RMS	root mean square
q_{cal}	theoretical NP uptake (mg/g)
q_{exp}	experimental NP uptake (mg/g)
K_D	desorption rate constant (s $^{-1}$)

Greek letters

α	$\int_0^t Cdt$, derived from the shrinking core model, defined in Eqs. (13) and (14) (Preetha and Viruthagirl, 2007)
α_P	Redlich–Peterson isotherm constant
β	Redlich–Peterson isotherm constant (dependent on the heterogeneity of the binding surface)

88 Chitosan, (1→4)-2-amino-2-deoxy- β -D-glucan, produced on an
 89 industrial scale by the alkaline deacetylation of chitin, one of the
 90 most abundant biopolymers in nature, was used in this study as
 91 the supporting material for living biomass immobilisation. It
 92 should be noted that the use of chitosan for living cell immobilisation
 93 has a limitation due to its anti-microbial activity (Helander
 94 et al., 2001). However, the fungal resting spores used in this study
 95 are tolerant to chitosan gelling because of their extra thick cell
 96 wall.

97 This study presents the biosorption characteristics of NP on
 98 dead chitosan-immobilised fungal beads, referred to as “dead
 99 beads”. Suitable isotherm and kinetic models fitted by non-linear
 100 regression using the ‘solver’ add-in with Microsoft Excel 2007 are
 101 proposed. Also, the reusability of the dead beads, that is the stability
 102 to repeated adsorption–desorption cycles, is discussed in reference
 103 to their feasibility for industrial use.

104 1.1. Adsorption equilibrium

105 The capacity of an adsorbent can be described by the equilibrium
 106 sorption isotherm, which is characterised by certain constants
 107 whose values express the surface properties and affinity of
 108 the adsorbent.

109 1.1.1. The Langmuir sorption isotherm

110 This model assumes an ideal, totally homogeneous adsorption
 111 surface with a finite number of binding sites and a few interactions
 112 between adsorbed molecules (Aksu and Balibek, 2007) is given by:

$$113 q = \frac{Q_0 b C_e}{1 + b C_e} \quad (1)$$

116 1.1.2. The Freundlich sorption isotherm

117 This model is suitable for a highly heterogeneous, energetic dis-
 118 tribution of active sites, with interactions between adsorbed mol-
 119 ecules (Aksu, 2001; Aksu et al., 2007), and is given by:

$$120 q = K_F C_e^{1/n} \quad (2)$$

121 1.1.3. The Redlich–Peterson sorption isotherm

122 This model is a combination of the Langmuir and Freundlich
 123 models and is given by Eq. (3). β lies between 0 and 1. For $\beta = 1$
 124 the Redlich–Peterson model converts to the Langmuir model
 125 (Aksu, 2001).

$$126 q = \frac{K_R C_e}{1 + a_R C_e^\beta} \quad (3)$$

127 1.1.4. The Fritz–Schlünder sorption isotherm

128 This isotherm for single-component systems more flexible to fit
 129 the experimental data since it contains more parameters than any
 130 other equilibrium isotherm (Fritz and Schluender, 1974; Yang and
 131 Al-Duri, 2005). It is usually written as:

$$132 q = \frac{K_S C_e^{b_1}}{1 + a_S C_e^{b_2}} \quad (4)$$

133 1.2. Adsorption kinetics

134 1.2.1. Kinetic models

135 Two simplified kinetic equations, from the pseudo first-order
 136 and pseudo second-order kinetic models initially proposed by Lager-
 137 ergren (1989) and Ho and McKay (2000), respectively, were used
 138 for a wide range of solute-sorbent systems.

139 1.2.1.1. Pseudo first-order kinetic model (Lagergren’s equation). This
 140 model assumes that the biosorption rate is proportional to the
 141 number of unoccupied sites on the biosorption surface (Ozdemir
 142 et al., 2003). The kinetic model based on solid capacity gives:

$$143 q = q_e (1 - e^{-K_1 t}) \quad (5)$$

144 1.2.1.2. Pseudo second-order kinetic model (Ho’s equation). This
 145 model assumes the driving force for adsorption rate comes from
 146 the square of the difference between q and q_e . It was transformed
 147 to non-linear form, giving as the equation:

156

$$q = \frac{q_e^2 K_2 t}{1 + q_e K_2 t} \quad (6)$$

159 **1.2.2. Diffusion models**

160 Sorption kinetics is generally controlled by various factors
 161 including (i) bulk diffusion, (ii) film diffusion (external mass transfer),
 162 (iii) intraparticle diffusion, and (iv) solute adsorption at active
 163 sites by the mechanisms of ion exchange, precipitation, complexation
 164 or chelation. Different diffusion models propose different diffusion
 165 kinetic mechanisms and rate-controlling steps.

166 **1.2.2.1. Intraparticle diffusion model.** The model implies that the dif-
 167 fusion from the surface to intraparticle sites is the only rate-limiting
 168 step (Yang and Al-Duri, 2005). The model can be expressed as:

$$q = k_p t^{0.5} \quad (7)$$

172 The half adsorption time $t^{0.5}$ is the time required for the adsorb-
 173 ent to take up half of the adsorbate it has at equilibrium. The rate
 174 constant, k_p obtained from the slope of Eq. (11), is related to the
 175 intraparticle diffusivity as:

$$k_p = \frac{6q_e}{R} \sqrt{\frac{D}{\pi}} \quad (8)$$

179 **1.2.2.2. Shrinking core model.** This model was applied to fluid-par-
 180 ticle chemical reactions (Lavenspiel, 1972) and, more specifically, to
 181 solute adsorption by ion exchange, precipitation, complexation
 182 and/or chelation. These processes are controlled by liquid film dif-
 183 fusion, with the extent of the sorption being a function of time gi-
 184 ven by:

$$X = \frac{3D}{\delta R C} \alpha \quad (9)$$

188 If the film diffusion is the rate determining process, a plot of X
 189 versus α will give a straight line (Preetha and Viruthagirl, 2007).
 190 If the process is the particle diffusion control, the model is repre-
 191 sented by:

$$F(X) = 1 - 3(1 - X)^{2/3} + 2(1 - X) = \frac{6D}{R^2 C_0} \alpha \quad (10)$$

195 Consequently, in this case, a plot of the function $F(X)$ versus α
 196 will give a linear relationship, and the diffusivity can be obtained
 197 from the slope of such a plot using (Preetha and Viruthagirl, 2007):

$$D = (\text{slope}) \frac{C^0 R^2}{6} \quad (11)$$

201 **Q3 2. Methods**202 **2.1. Materials**203 **2.1.1. Chemicals**

204 NP was purchased from Fluka Chemical Industries, Ltd. It was a
 205 mixture of isomers and used without further purification. Chitosan
 206 was a gift from TC Union Company, Thailand. All other chemicals
 207 used were of reagent grade.

208 **2.1.2. Microorganisms**

209 Five fungal strains, i.e. *Rhizopus arrhizus* TISTR 3606, *R. arrhizus*
 210 TISTR 3610, *Trichoderma harzianum*, *Aspergillus oryzae* and *Penicil-
 211 lium* sp., available from a microbiological laboratory of Faculty of
 212 Liberal Arts and Science, Kasetsart University, were used in this
 213 work.

214 **2.1.3. Instruments**

215 Absorbance spectra were recorded on an Ultrospec 3000 UV-vis
 216 spectrometer. Freeze-dried samples were prepared using a Bio-
 217 freezer and DW 3 Lyophilyzer (Scientific promotion Co., Ltd.).

218 **2.2. Methods**219 **2.2.1. Preparation of fungal biomass for NP biosorption**

220 The five fungal strains were inoculated separately into a growth
 221 medium, Tryptone glucose yeast extract (TCY), composed of yeast
 222 extract (10 g/L), peptone (20 g/L) and dextrose (20 g/L) in distilled
 223 deionised water and cultivated in rotary shaking flasks for 4 days.
 224 The biomasses were autoclaved at 121.5 °C for 15 min and then
 225 harvested by filtering through a membrane filter. These were then
 226 washed thoroughly with deionised water and freeze-dried. Each
 227 sample of dried dead biomass was ground using a mortar and pestle.
 228 Particles passing through a 210 µm sieve were used as fungal
 229 powder for NP biosorption.

230 **2.2.2. Pre-treatment of biomass**

231 Five-day old living biomass samples, 5 g wet weight, were pre-
 232 treated in six different ways: exposure to acid, basic or organic
 233 solution, in combination with and without heat treatment as fol-
 234 lowings: (i) washed and freeze-dried (untreated), (ii) washed and
 235 autoclaved for 15 min at 121 °C, (iii) immersed in a 1 M H₂SO₄
 236 for 1 h washed and freeze-dried, (iv) immersed in a 2 N NaOH for
 237 1 h, washed and autoclaved at 121 °C for 15 min, (v) immersed in
 238 a 2 N NaOH and autoclaved at 121 °C for 15 min, (vi) immersed
 239 in a 10% formaldehyde for 1 h, washed and freeze-dried and (vii)
 240 spread on a membrane filter and dried at 50 °C for 24 h. The treated
 241 fungal biomass was then dried and ground according to the above
 242 method 2.2.1. The NP biosorption ability of pre-treated samples
 243 was also compared with activated charcoal and commercial chito-
 244 san powder.

245 **2.2.3. Biosorption study**

246 Stock solution of **nonylphenol** (1.00 g/L) was prepared in meth-
 247 anol and stored under dark conditions. Fungal powder (0.02 g,
 248 duplicate samples) was added to 20 mL of the 100 mg/L of NP sol-
 249 ubilised in 10% methanol in 125 mL conical flasks. The flasks were
 250 placed on a rotary shaker (100 rpm, 30 °C) for 1 h. Each mixture
 251 was filtered through a membrane filter (Whatman No.1), and then
 252 extracted with dichloromethane (20 mL) for NP determination. The
 253 concentration of NP in the organic layer was determined by com-
 254 paring absorbance at a wavelength of 275 nm to a standard curve
 255 using dichloromethane as a solvent. The NP uptake was calculated
 256 by using:

$$q = \frac{(C_0 - C) * V}{M} \quad (12)$$

257 In order to optimize the pH for maximum removal efficiency,
 258 experiments are conducted in the pH range from 2.0 to 10.0 using
 259 0.02 g of *R. arrhizus* TISTR 3610 biomass with 20 mL of 100 mg
 260 nonylphenol/L solutions at room temperature. pH of the adsorbate
 261 solution is adjusted to set value with 0.01 M HCl and 0.01 M NaOH
 262 at the start of the experiment. It is confirmed through the prelimin-
 263 ar experiments that the 6 h is sufficient to attain equilibrium be-
 264 tween adsorbent and adsorbate. Each experiment is repeated twice
 265 and mean values are taken.

266 **2.2.4. Preparation of the dead beads**

267 The entrapment of *R. arrhizus* TISTR 3610 sporangiospores pro-
 268 duced immobilised fungal bead biosorbents. Chitosan (2 g) was
 269 dissolved in acetic acid solution (3% v/v, 9.9 mL), aseptically heated
 270 at 100 °C for 5 min, then cooled and mixed with the *R. arrhizus*
 271

273 spore suspension (0.1 mL, about 3.7×10^9 spores/mL). The chitosan suspension was added dropwise to sterilised sodium tri-poly-
 274 phosphate (2% w/v, 100 mL) and let stand for 3 h to yield stable
 275 2 mm diameter beads which were washed several times with
 276 deionised distilled water. The beads with trapped spores were
 277 transferred into TGY medium and incubated on a rotary shaker
 278 (100 rpm) at 30 °C for 5 days. After this, the chitosan beads with
 279 immobilised fungal mycelia were inactivated by autoclaving at
 280 121 °C for 15 min, removed from the medium by filtration, washed
 281 with distilled water and freeze-dried.

283 2.2.5. SEM studies

284 The cross-section and surface of the fungus immobilised beads
 285 were observed by SEM using the preparation method of Pluemsab
 286 et al. (2007).

287 2.2.6. Batch kinetic experiments

288 Kinetic experiments were performed in continuously stirred
 289 flasks (100 rpm at 30 °C) containing 100 mL NP solution at different
 290 concentrations (50–300 mg/L) and 0.1 g of the dead beads. Optimal solution pH was adjusted to 6.5–7.0, since NP is removed
 291 more effectively by *R. arrhizus* TISTR 3610 biomass. Two milliliters
 292 of samples were withdrawn at regular intervals and extracted with
 293 dichloromethane (2 mL). The organic layer was collected by centrifuging
 294 at 3500 rpm at 4 °C. The residual NP concentration was
 295 determined by UV/vis spectroscopy at 275 nm (Ultrospec 3000,
 296 Pharmacia Biotech Inc., Thailand). This was done for duplicate samples
 297 of each treatment.

298 The validity of the isotherm and kinetic models were checked
 299 by plotting Eqs. (1)–(11) with the observed data. The kinetic
 300 parameters involved in the models were estimated using non-linear
 301 regression analysis. By trial and error, and using the solver add-in
 302 with Microsoft Excel spreadsheet application, the kinetic parameters
 303 were determined by minimising the difference between the
 304 experimental data and fitted model.

306 2.2.7. Desorption studies

307 Desorption studies were conducted in methanol with equilibrium
 308 being reached within 90 min. Initially, a known weight of
 309 dead beads was placed in 100 mg/L NP solution overnight, and the
 310 NP adsorbed determined from the difference between the initial
 311 and final NP concentration. The beads were separated from the
 312 solution by vacuum filtration.

313 The NP-beads were mixed with methanol and kept in sealed
 314 flasks placed in a shaker at 30 °C overnight. The amount of NP desorbed
 315 was determined by UV/vis absorbance at 275 nm of wavelength.
 316 Various desorption kinetic models were considered and
 317 compared against the experimental data for fit. The desorption
 318 process was repeated five times to check repeatability.

319 The desorption ratio was calculated from the amount of NP adsorbed
 320 on the biomass and the final NP concentration in desorption
 321 medium, that is:

$$324 \text{Desorption ratio} = \frac{\text{Release nonylphenol (mg)}}{\text{Initially sorbed nonylphenol (mg)}} \times 100 \quad (13)$$

325 2.2.8. Statistical analyses

326 The fit of kinetic expressions to the experimental data was
 327 tested using the value of coefficient of determination, r^2 (Kumar,
 328 2007), which is defined as:

$$331 r^2 = \frac{\sum (q_{\text{cal}} - \bar{q}_{\text{exp}})^2}{\sum (q_{\text{cal}} - \bar{q}_{\text{exp}})^2 + \sum (q_{\text{cal}} - q_{\text{exp}})^2} \quad (14)$$

332 Also used was the non-normalised root mean square (RMS) that
 333 weights the actual error at all points (Yang and Al-Duri, 2005), and
 334 is defined as:

$$335 \text{Non-normalised RMS} = \sqrt{\frac{\sum_{i=1}^N (q_{\text{cal}} - q_{\text{exp}})^2}{N}} \quad (15)$$

336 All statistical data analysis was performed with the help of the tool-
 337 box present in Microsoft® Excel (Microsoft Corporation, USA).

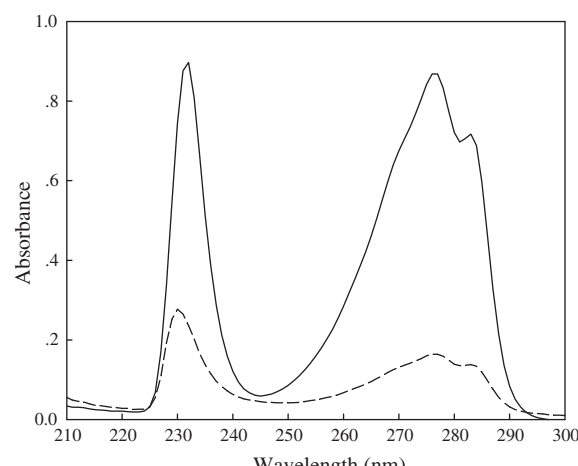
3. Results and discussion

340 3.1. Screening of fungal biomass for NP biosorption

341 Five fungal strains, obtained from the culture collection in a laboratory of the Faculty of Liberal Arts and Science, Kasetsart University, were used for the NP biosorption study. Since NP solubility in water is extremely low (5.43 mg/L at 20 °C) (Kim et al., 2005), it was extracted from the water layer with dichloromethane before analyses. From an initial concentration of 50 mg/L, the amount of NP absorbed in each fungal mycelia was similar, about 69–76%, as follows: $68.8 \pm 2.1\%$ for *R. arrhizus* TISTR 3606, $75.9 \pm 0.6\%$ for *R. arrhizus* TISTR 3610, $70.6 \pm 2.1\%$ for *T. harzatum*, $70.5 \pm 0.6\%$ for *A. oryzae*, and $69 \pm 4\%$ for *Penicillium* sp. The UV-vis spectra showed decreases in all three main peaks of NP isomer (Fig. 1). The most effective NP absorbent was the mycelia of *R. arrhizus* TISTR 3610, therefore it was selected as a model of the fungal strains for NP biosorption in this work. Also investigated was the use of non-viable and viable *R. arrhizus* biomass to remove phenol and its derivatives from aqueous solutions in batch reactors (Tsezos and Bell, 1989).

358 3.2. Pre-treatment of fungal biomass and solution pH for NP biosorption

359 Research has shown that some physical or chemical pre-treatment processes can facilitate more efficient uptake of sorbate as compared to untreated biomass. Six pre-treatments of mycelial biomass of *R. arrhizus* were prepared to observe various chemical and physical effects on both cell walls and intracellular compartments. Heat treatment by autoclave at 121 °C for 15 min was found to be the most effective for biosorption with an uptake of 73.7 ± 1.0 mg NP/g (Table 1). Treatments with drying at 50 °C for 24 h or soaking in 10% (v/v) formaldehyde for 1 h were also fairly effective, with NP uptakes larger than that of untreated biomass at 54 ± 12 mg NP/g. However, the chemical treatments with strong



370 Fig. 1. Typical UV-vis spectrum of NP before (–) and after (---) treatment with
 371 fungal grill for 1 h.

Table 1

Nonylphenol^a biosorption of *Rhizopus arrhizus* TISTR 3610 treated with different mycelial preparations.

Biomass/biosorbent	NP uptake (mg/g)
<i>Pre-treatment</i>	
Untreated	54.4 ± 11.9
Autoclaved (121 °C, 15 min)	73.7 ± 1.0
1 M H ₂ SO ₄ for 1 h	49.8 ± 5.1
1 N NaOH for 1 h	37.1 ± 0.0
1 N NaOH at 121 °C for 15 min	4.5 ± 3.4
10% (v/v) formaldehyde for 1 h	68.3 ± 0.4
Dried at 50 °C for 24 h	61.2 ± 7.9
<i>Commercial biosorbents</i>	
Activated charcoal	83.1 ± 0.0
Chitosan	56.3 ± 0.1

^a Initial NP concentration of 100 mg/L, performed at 100 rpm, at 30 °C for 1 h.

acid or strong base reduced the NP absorption capacity. It could be concluded that the surface modification *in situ* by the pH of these pre-treatments are not appropriate for increased biosorption of this hydrophobic aromatic compound. Therefore, the pre-treatment in the autoclave was selected for the next biosorbent preparation, giving adsorption comparable with the two frequently used commercial biosorbents, activated charcoal (83.1 ± 0.0 mg NP/g) and chitosan (56.3 ± 0.1 mg NP/g) (Table 1).

Biosorption of NP exhibited an uptake capacity over 78% and 85% with wide initial pH ranges of 3.1–10.0 and 5.7–7.5, respectively. Maximal NP removal of 87% was obtained at an initial pH 6.6. At initial pH 2.3, however, the NP uptake decreased to 62%. pH solutions at equilibrium under specified conditions in this work were found approximately to decrease from 5.7–7.5 to 4.0–4.9. Accordingly, NP are considered to be molecular form in the range of pH ≤ 7.0 (its *pK_a* = 10.28) (Fan et al., 2008). Therefore, NP effectively adsorbed onto fungal biomass in the form of molecules rather than phenolate anion derivatives. The molecular interactions, i.e. hydrogen bonding, hydrophobic interaction and Van der Waals forces could play an important role for the NP adsorption. Neither positive nor negative charges resulting from the biosorbent and pH solution is attractive through electrostatic force for NP biosorption. Nadavala et al. (2009) described both phenol and *o*-chlorophenol existing predominantly as neutral species at pH 7.0. Their interaction with the chitosan–calcium alginate blended beads is considered mainly as non-polar, and the forces responsible for adsorption are physical van der Waals forces.

3.3. Properties of the dead beads

There are a number of immobilisation methods using dead grinded fungal biomass encapsulated in polymer matrix, including calcium alginate and polyvinyl alcohol (Wu and Yu, 2007). In the present study, asexual spores of *R. arrhizus* were trapped into chitosan beads by a liquid curing method in the presence of TPP, and then cultivated for 5 days for complete spore germination. After this period, the hyphae would convert to a sporulation cycle. The bead surface was found to have homogeneously distributed exuberant mycelia inside, and outward growing mycelia covering the whole particle surface. The dry weight of immobilised fungus in the support was 9.7 × 10⁻⁴ g/bead. The dried chitosan-immobilised fungal beads had a diameter of approximately 4 mm with a spherical shape which was completely different from the 1–1.5 mm diameter dried plain beads. It also improves the affinity of the biosorbent for the solute by providing directly exposure without any barriers. The dead beads were also stronger and more stable than plain chitosan beads when immersed in acid solution (data not shown), even at pH 1.

3.4. Evaluation of adsorption isotherms

To model NP biosorption and gain a better understanding of the sorption process, the four adsorption isotherms, Eqs. (1)–(4) were compared to the experimental data for fit. The adsorption isotherm constants with the corresponding correlation coefficients, Eq. (14) and non-normalised RMS, Eq. (15) for each model are presented in Table 2. Although linear regression has been the most commonly used method to obtain the parameters and determine the fit of the kinetic expressions, non-linear regression provides a better measure of fit (Kumar, 2007). As compared to non-linear analysis, the correlation coefficients (*r*²) of 0.8912 (Redlich–Peterson), 0.9320 (Freundlich) and 0.7561 (Langmuir), except that for the non-linearized Fritz–Schlünder, were obtained from the fitting parameters by linear regression. From the results shown in Table 2, the four-parameter isotherm models of Fritz–Schlünder gave the best fit with *r*² = 0.9984, followed by the three- and two-parameter isotherm models of Redlich–Peterson (*r*² = 0.9302), Freundlich (*r*² = 0.9287) and Langmuir (*r*² = 0.9271). Yang and Al-Duri (2005) also observed the superiority of the Fritz–Schlünder model over the other models for biosorption of three reactive dyes onto activated carbon. Based on the Freundlich isotherm plot, the adsorption capacity (*K_F*) was found to be 30.25 mg/g with an adsorption intensity (*n*) of 1.87. These were similar values to those for the biosorption of pentachlorophenol onto live *R. arrhizus* which has a *K_F* of 32.13 mg/g and *n* of 1.79 (Tsezos and Bell, 1989). The high value of the maximum adsorption capacity, *Q₀* of 312.17 mg/g and the low value of the Langmuir constant, *b* of 0.05 L/mg were obtained with the Langmuir isotherm. In general, a small value of *b* indicates that the adsorbate has a high binding affinity for the biosorbent (Arica et al., 2003). A similar observation was reported for 2,4-dichlorophenol biosorption onto free and calcium alginate immobilised biomass of white-rot fungus *Phanerochaete chrysosporium* with *b* values of 0.039 and 0.053 L/mg, respectively (Wu and Yu, 2007). The values of *K_F* and *Q₀* also indicate the great affinity for NP by the beads in this study.

Table 2

Parameters from fitting the adsorption equilibrium data to various isotherm models.

Langmuir constants	
<i>Q₀</i> (mg/g)	312.17
<i>b</i> (L/mg)	0.05
<i>r</i> ²	0.9271
Non-normalised RMS	20.4009
Freundlich constants	
<i>K_F</i>	30.25
<i>N</i>	1.87
<i>r</i> ²	0.9287
Non-normalised RMS	18.5402
Redlich–Peterson constants	
<i>K_R</i>	180.94
<i>α_P</i>	5.26
<i>β</i>	0.49
<i>r</i> ²	0.9302
Non-normalised RMS	18.4794
Fritz–Schluender constants	
<i>K_S</i>	46.87
<i>a_s</i>	0.67
<i>b₁</i>	0.74
<i>b₂</i>	0.35
<i>K_S/a_s</i>	70.47
<i>r</i> ²	0.9984
Non-normalised RMS	18.4617

Note: Parameters determined using non-linear regression in Microsoft® Excel (Microsoft Corporation, USA).

Table 3

Kinetic parameters for pseudo first-order and pseudo second-order biosorption and desorption of NP using dead beads.

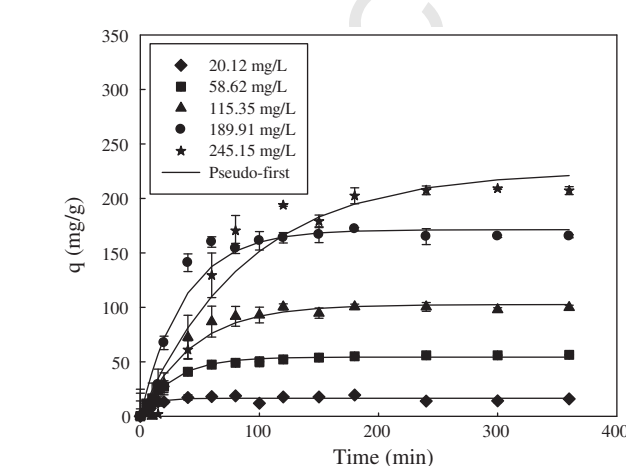
	Nonylphenol		Pseudo first-order rate			Pseudo second-order rate				
	C_0 (mg/L)	q (mg/g)	K_1 (min ⁻¹)	q_e (mg/g)	r^2	Non-normalised RMS	K_2 (g/mg min)	q_e (mg/g)	r^2	Non-normalised RMS
Biosorption	20.1156	19.4558	0.10227	16.4679	0.6726	2.0072	1.03×10^{-2}	17.2494	0.5742	2.2347
	58.6191	55.9184	0.03606	54.3062	0.9878	1.7437	7.41×10^{-4}	61.3428	0.9921	1.3298
	115.3538	100.5443	0.02267	102.5006	0.9107	10.2708	1.91×10^{-4}	122.9755	0.8635	12.7894
	189.9116	171.9728	0.02705	171.2495	0.9150	16.1795	1.47×10^{-4}	200.9999	0.8753	21.0549
	245.1497	207.4150	0.01119	224.9302	0.8597	30.8957	1.76×10^{-5}	338.0162	0.6926	50.3715
Desorption	–	145.6420	0.40945	138.1793	0.5655	29.5331	4.98×10^{-3}	145.8314	0.9997	5.2708

Note: Parameters determined using non-linear regression in Microsoft® Excel (Microsoft Corporation, USA).

455

3.5. Evaluation of adsorption kinetics

456 The rate constants for the pseudo first-order (K_1) and pseudo
 457 second-order (K_2) sorption reactions were obtained by plotting
 458 the non-linear curves fitting Eqs. (5) and (6). Kinetic rate constants
 459 for NP uptake by the dead beads are presented in Table 3. From the
 460 correlation coefficients, the experimental adsorption data gave a
 461 better fit to pseudo first-order in the concentration range of
 462 58.62 – 189.91 mg/L. The corresponding kinetic models are plotted
 463 in Fig. 2. Using Eq. (7), the plots of intraparticle diffusion with NP
 464 uptake versus t at different initial NP concentrations (20.12 –
 465 245.15 mg/L) are shown in Fig. 3. The plots were not linear over
 466 the whole time range, implying that more than one process af-
 467 fected the adsorption. Three linear regions better describe the
 468 intraparticle diffusion when the initial concentration of NP was
 469 in the range 58.62 – 245.15 mg/L. The initial linear sections have
 470 steeper slopes than the subsequent sections. The multi-linearity
 471 of the plots can be compared to the three steps of acid dye adsorp-
 472 tion onto chitosan reported by Cheung et al. (2007). The first, stee-
 473 per section was attributed to the diffusion of solute through the
 474 solution to the external surface of the adsorbent, or the boundary
 475 layer diffusion of solute molecules. The second section was attrib-
 476 uted to the gradual adsorption stage with diffusion into the mesop-
 477 ores, where intraparticle diffusion was the rate limiting process.
 478 The third portion was attributed to the final equilibrium stage
 479 for which the intraparticle diffusion started to slow due to the
 480 extremely low solute concentration remaining in the solution, and
 481 relates to adsorption of the solute into micropores. The slopes of
 482 the linear sections indicate the rates of adsorption, a shallower
 483 slope corresponding to a slower adsorption process. Thus, it can
 484 be implied that the rate-controlling step of NP adsorption was
 485 essentially intraparticle diffusion. In addition, relatively low to
 486

**Fig. 2.** Adsorption kinetics of nonylphenol by the dead beads described with the pseudo first-order model Eq. (5).

Please cite this article in press as: Lang, W., et al. Biosorption of nonylphenol on dead biomass of *Rhizopus arrhizus* encapsulated in chitosan beads. *Bior-
 esour. Technol.* (2009), doi:10.1016/j.biortech.2009.06.021

487 moderate levels of initial NP concentration (20.12 – 189.91 mg/L) 488 induced adsorption into micropores as observed from the nearly 489 parallel third section of the plots. The intraparticle diffusivity (D) 490 and intraparticle diffusion rate constant (k_p) significantly increase 491 with increased initial NP concentration (Table 4). On the other 492 hand, using a shrinking core model and plotting $R(X)$ against α 493 shows significant linear relationships (Fig. 4b), as compared to 494 plotting X against α (Fig. 4a). The diffusivity values are in the range 495 of 2.37×10^{-4} – 1.89×10^{-4} cm² s⁻¹. Clearly, this implies that 496 intraparticle diffusion is the rate-controlling step for the NP bio- 497 sorption in this work. Although intraparticle diffusion and shrink- 498 ing core models can describe the biosorption process for NP uptake 499 by the dead beads reasonably well, an initial NP concentration was 500 quite limited lower than approximately 200 mg/g (Fig. 4).

3.6. Desorption kinetics

501 Desorption studies elucidate the mechanism of adsorption and 502 recovery of NP from water, its interaction with the adsorbent. 503 The adsorbed NP remains mostly stable on the adsorbent and can 504 be desorbed using methanol. It can be seen that the desorption 505 process of NP can well be described by a pseudo second-order model 506 using a non-linear regression method (Fig. 5). This was evident 507 from the high r^2 value of 0.9997 and low non-normalised RMS 508 value of 5.2708 as shown in Table 3. NP desorption by methanol also 509 occurred rapidly ($K_2 = 4.98 \times 10^{-3}$ g/mg min). Although, it has 510 been reported that distilled water (Wu and Yu, 2007), CaCl₂ solution 511 (Benoit et al., 1998) and NaNO₃ solution (Daughney and Fein, 512 1998) can be used to desorb solutes from phenol-loaded and chloro- 513 phenol-loaded biomass, using methanol as the desorbing agent 514 allows for easy regeneration as it can be separated from nonylphenol 515 by vapourisation. The NP waste can then be further degraded 516

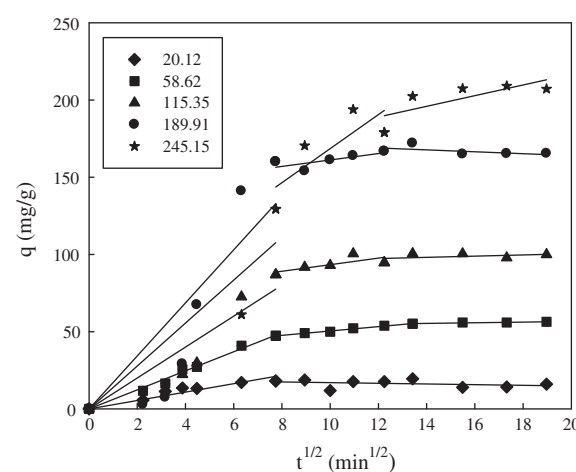
**Fig. 3.** Intraparticle diffusion kinetics for nonylphenol biosorption on the dead beads (multi-linearity) described with Eq. (7).

Table 4

Intraparticle diffusion and shrinking core coefficients.

Initial concentration of NP (mg/L)	Intraparticle diffusion			Shrinking core model		
	Slope	k_p mg/(g min ^{0.5})	Diffusion coefficient (cm ² /s)	Slope	C^0 (mg/L)	Diffusion coefficient (cm ² /s)
20.12	1.21	9.79×10^1	0.15	1.89×10^{-3}	1.03	2.37×10^{-4}
58.62	3.76	9.32×10^2	1.67	5.89×10^{-4}	2.95	2.80×10^{-4}
115.35	8.38	3.30×10^3	6.50	4.41×10^{-4}	5.30	3.65×10^{-4}
189.91	12.30	8.80×10^3	15.75	2.21×10^{-4}	9.07	2.98×10^{-4}
245.15	14.70	1.31×10^4	24.01	1.22×10^{-4}	10.94	1.89×10^{-4}

Bead dosage = 0.1 g, NP solution volume = 100 mL, bead amount = 18 beads.

Note: Parameters determined using non-linear regression in Microsoft® Excel (Microsoft Corporation, USA).

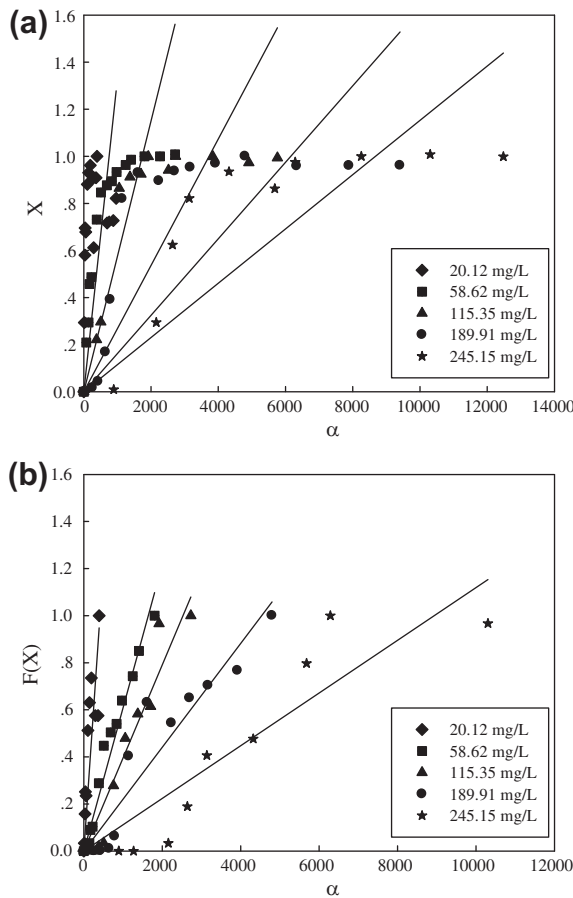


Fig. 4. Shrinking core model for (a) external film diffusion control and (b) particle diffusion control.

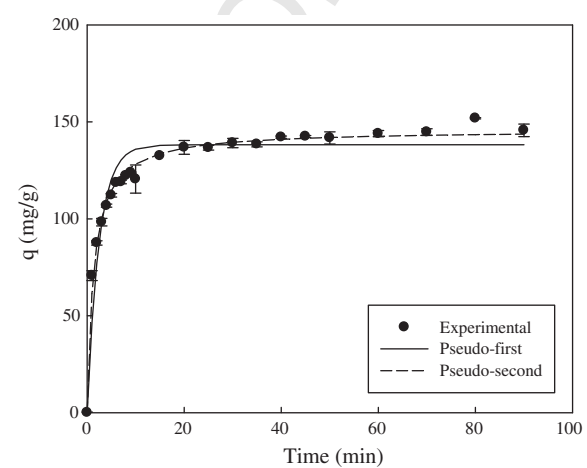


Fig. 5. Comparison of two desorption kinetic models for NP removal by the dead beads. Curve fitting performed with SigmaPlot 11.0 (Systat Software Inc., USA).

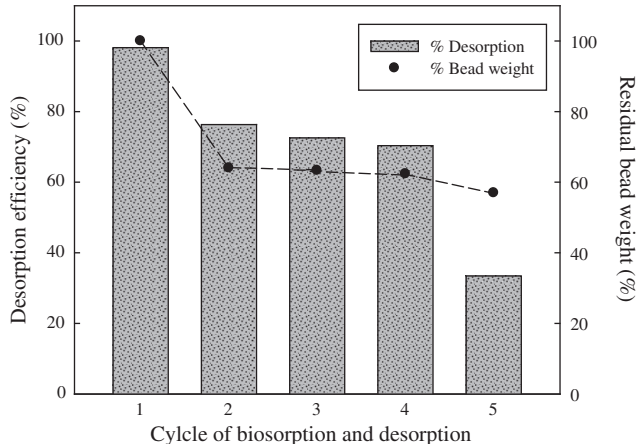


Fig. 6. Desorption efficiency of the dead beads after repeated NP biosorption and NP desorption with methanol.

516 by chemical or physical treatments (Maniero et al., 2008). The
 517 regenerated dead beads are also reusable and, from this study, active
 518 in four batches (Fig. 6). The weight loss of dead beads was 43%
 519 by the end of the fifth batch use.

520 4. Conclusion

521 The use of chitosan-immobilised beads was effective for an
 522 innovative treatment of low soluble recalcitrant pollutant from
 523 wastewater. The fungal dead biomass could be prepared readily
 524 on a commercial scale as an alternative low-cost biosorbent for
 525 use in wastewater treatment plants. In this work, the dead beads
 526 were pre-treated with moist heat which substantially increased
 527 their capacity of NP biosorption. Equilibrated NP adsorption with
 528 the dead beads best fitted the Fritz-Schlünder isotherm. A max-

imal monolayer capacity of the dead beads was over 312 mg/g. The rate of NP biosorption was rapid in the first 40 min of contact time. The kinetics for adsorption of NP onto the dead beads was well described by the pseudo first-order equation, while that for desorption was well described by the pseudo second-order one. Both intraparticle diffusion and shrinking core models were found suitably consistent with the adsorption experimental data, especially at the NP concentration less than 200 mg/L. The regeneration of used dead beads with methanol was effective for at least 4 batch cycles in this study. As mentioned, the production of the dead beads and their possible reuses provides an alterna-

540 tive biosorbent for NP removal, as well as for other hydrophobic
 541 aromatic recalcitrant pollutants in wastewater.

542 5. Uncited references

543 Ho and Mckay (1999), Kapoor and Viraraghavan (1998) and
 544 Q1 Singh et al. (2008).

545 Acknowledgements

546 This work was supported by Thailand Research Fund (TRF) under
 547 the research grants "MRG5080420" and "**RPUS-I251A13001**"
 548 awarded in 2007 and 2008, respectively. The authors are grateful
 549 to the Faculty of Liberal Arts and Science and the Faculty of
 550 Agro-Industry, Kasetsart University, for facilitating the research,
 551 and additional Wilhelm J. Holzschuh of the Faculty for proof reading
 552 the manuscript.

553 References

554 Ahel, M., McEvoy, J., Giger, W., 1993. Bioaccumulation of the lipophilic metabolites
 555 of nonionic surfactants in freshwater organisms. *Environ. Pollut.* 79, 243–248.

556 Aksu, Z., 2001. Biosorption of reactive dyes by dried activated sludge: equilibrium
 557 and kinetic modeling. *Biochem. Eng. J.* 7, 79–84.

558 Aksu, Z., 2005. Application of biosorption for the removal of organic pollutants: a
 559 review. *Process Biochem.* 40, 997–1026.

560 Aksu, Z., Balibek, E., 2007. Chromium (VI) biosorption by dried *Rhizopus arrhizus*:
 561 effect of salt (NaCl) concentration on equilibrium and kinetic parameters. *J.
 562 Hazard. Mater.* 145, 210–220.

563 Asku, Z., Cagatay, S.S., Gönen, F., 2007. Continuous fixed bed biosorption of reactive
 564 dyes by *Rhizopus arrhizus*: determination of column capacity. *J. Hazard. Mater.*
 565 143, 362–371.

566 Arica, M.Y., Arpa, Ç., Ergene, A., Bayramoğlu, G., Genç, Ö., 2003. Ca-alginate as a
 567 supper for Pb(II) and Zn(II) biosorption with immobilized *Phanerochaete
 568 chrysosporium*. *Carbohyd. Polym.* 52, 167–174.

569 Benoit, P., Barriuso, E., Calvet, R., 1998. Biosorption characterization of herbicides,
 570 2,4-D and atrazine, and two chlorophenols on fungal mycelium. *Chemosphere*
 571 37, 1271–1282.

572 Cheung, W.H., Szeto, Y.S., Mckay, G., 2007. Intraparticle diffusion processes during
 573 acid dye adsorption onto chitosan. *Bioresour. Technol.* 98, 2897–2904.

574 Daughney, C.J., Fein, J.B., 1998. Sorption of 2,4,6-trichlorophenol by *Bacillus subtilis*.
 575 *Environ. Sci. Technol.* 32, 749–752.

576 Ekelund, R., Bergman, A., Granmo, A., Berggren, M., 1990. Bioaccumulation of 4-
 577 nonylphenol in marine animals. A re-evaluation. *Environ. Pollut.* 64, 107–120.

578 Fan, J., Fan, Y., Pei, Y., Wu, K., Wang, J., Fan, M., 2008. Solvent extraction of selected
 579 endocrine-disrupting phenols using ionic liquids. *Sep. Purif. Technol.* 61, 324–
 580 331.

581 Fritz, W., Schluender, E.V., 1974. Simultaneous adsorption equilibria of organic
 582 solutes in dilute aqueous solutions on activated carbon. *Chem. Eng. Sci.* 29,
 583 1279–1282.

584 Fu, Y., Viraraghavan, T., 2001. Fungal decolorization of dye wastewaters: a review.
 585 *Bioresour. Technol.* 79, 251–262.

586 Granmo, A., Ekelund, R., Magnusson, K., Berggren, M., 1989. Lethal and sublethal
 587 toxicity of 4-nonylphenol to the common mussel. *Environ. Pollut.* 59, 115–127.

588 Helander, I.M., Nurmiaho-Lassila, E.L., Ahvenainen, R., Rhoades, J., Roller, S., 2001.
 589 Chitosan disrupts the barrier properties of the outer membrane of gram-
 590 negative bacteria. *Int. J. Food Microbiol.* 71, 235–244.

591 Ho, Y.S., Mckay, G., 1999. Pseudo second-order model for sorption processes.
 592 *Process Biochem.* 34, 451–465.

593 Ho, Y.S., Mckay, G., 2000. The kinetics of sorption of divalent metal ions onto
 594 sphagnum moss peat. *Water Res.* 34, 735–742.

595 Kapoor, A., Viraraghavan, T., 1995. Fungal biosorption – an alternative treatment
 596 option for heavy metal bearing wastewaters: a review. *Bioresour. Technol.* 53,
 597 195–206.

598 Kapoor, A., Viraraghavan, T., 1998. Removal of heavy metals from aqueous solutions
 599 using immobilized fungal biomass in continuous mode. *Water Res.* 32, 1968–
 600 1977.

601 Kawasaki, N., Araki, M., Nakamura, T., Tanada, S., 2001. Inclusion behavior of 4-
 602 nonylphenol into cyclodextrin derivatives. *J. Colloid Interf. Sci.* 238, 215–218.

603 Kim, J., Korshin, G.V., Veliuchenko, A.B., 2005. Comparative study of electrochemical
 604 degradation and ozonation of nonylphenol. *Water Res.* 39, 2527–2534.

605 Kumar, K.V., 2007. Pseudo second-order models for the adsorption of safranin onto
 606 activated carbon: comparison of linear and non-linear regression methods. *J.
 607 Hazard. Mater.* 142, 564–567.

608 Lagergren, S., 1989. About the theory of so-called adsorption of soluble substances.
 609 *Kungliga Svenska Vetenskapsakademiens Handlingar*, Band 24, 1–39.

610 Lavenspiel, O., 1972. *Chemical Reaction Engineering*, second ed. John Wiley & Sons.
 611 pp. 21–32, 69–71, 357–408.

612 Maniero, M.G., Bila, D.M., Dezotti, M., 2008. Degradation and estrogenic activity
 613 removal of 17 β -estradiol and 17 α -ethinylestradiol by ozonation and O₃/H₂O₂.
 614 *Sci. Total Environ.* 407, 105–115.

615 Nadavala, K.S., Swayampakula, K., Boddu, M.V., Abburi, K., 2009. Biosorption of
 616 phenol and o-chlorophenol from aqueous solutions on to chitosan-calcium
 617 alginate blended beads. *J. Hazard. Mater.* 162, 482–489.

618 Nakada, N., Tanishima, T., Shinohara, H., Kiri, K., Takada, H., 2006. Pharmaceutical
 619 chemicals and endocrine disrupters in municipal wastewater in Tokyo and their
 620 removal during activated sludge treatment. *Water Res.* 40, 3297–3303.

621 Nevskaia, D.M., Guerrero-Ruiz, A., 2001. Comparative study of the adsorption from
 622 aqueous solutions and the desorption of phenol and nonylphenol substrates on
 623 activated carbons. *J. Colloid Interf. Sci.* 234, 316–321.

624 Pluemsab, W., Fukazawa, Y., Furuike, T., Nodasaka, Y., Sakairi, N., 2007.
 625 Cyclodextrin-linked alginate beads as supporting materials for *Sphingomonas
 626 cloacae*, a nonylphenol degrading bacteria. *Bioresour. Technol.* 98, 2076–2081.

627 Preetha, B., Viruthagiril, T., 2007. Batch and continuous biosorption of chromium (VI)
 628 by *Rhizopus arrhizus*. *Sep. Purif. Technol.* 57, 126–133.

629 Singh, A., Kumar, D., Gaur, J.P., 2008. Removal of Cu(II) and Pb(II) by *Pithophora
 630 oedogonia*: sorption, desorption and repeated use of the biomass. *J. Hazard.
 631 Mater.* 152, 1011–1019.

632 Tsezos, M., Bell, J.P., 1989. Comparison of the biosorption and desorption of
 633 hazardous organic pollutants by live and dead biomass. *Water Res.* 23, 561–
 634 568.

635 Wu, J., Yu, H.Q., 2007. Biosorption of 2,4-dichlorophenol by immobilized white-rot
 636 fungus *Phanerochaete chrysosporium* from aqueous solutions. *Bioresour.
 637 Technol.* 98 (2), 253–259.

638 Yang, X.Y., Al-Duri, B., 2005. Kinetic modeling of liquid-phase adsorption of reactive
 639 dyes on activated carbon. *J. Colloid Interf. Sci.* 287, 25–34.